

The Study of Weave-Pattern Effect on Filtration Performance of Woven Filter Cloths
by Computational Fluid Dynamic Modeling



A Thesis Submitted in Partial Fulfillment of the Requirements
for the Degree of Master of Engineering in Chemical Engineering
Department of Chemical Engineering
FACULTY OF ENGINEERING
Chulalongkorn University
Academic Year 2022
Copyright of Chulalongkorn University

การศึกษาผลของรูปแบบการถักทอของหน้ากากผ้าต่อประสิทธิภาพการกรองโดยวิธีการจำลอง
พลศาสตร์ของไหลเชิงคำนวณ



วิทยานิพนธ์นี้เป็นส่วนหนึ่งของการศึกษาตามหลักสูตรปริญญาวิศวกรรมศาสตรมหาบัณฑิต
สาขาวิชาวิศวกรรมเคมี ภาควิชาวิศวกรรมเคมี
คณะวิศวกรรมศาสตร์ จุฬาลงกรณ์มหาวิทยาลัย
ปีการศึกษา 2565
ลิขสิทธิ์ของจุฬาลงกรณ์มหาวิทยาลัย

วิศิษฐ์ บรรดาศักดิ์ : การศึกษาผลของรูปแบบการถักทอของหน้ากากผ้าต่อประสิทธิภาพการกรองโดยวิธีการจำลองพลศาสตร์ของไหลเชิงคำนวณ. (The Study of Weave-Pattern Effect on Filtration Performance of Woven Filter Cloths by Computational Fluid Dynamic Modeling) อ.ที่ปรึกษาหลัก : ผศ. ดร.พิมพ์พร พลเพชร

มลพิษทางอากาศเป็นปัญหาที่สำคัญทั่วโลก เนื่องจากการออกกำลังกายหรือกิจกรรมกลางแจ้งมีความสำคัญต่อสุขภาพที่ดีของมนุษย์นั้น แต่การทำกิจกรรมกลางแจ้งนั้นจะส่งผลกระทบต่อสุขภาพของมนุษย์และสิ่งแวดล้อมได้อย่างมากมาย เช่น จาก $PM_{2.5}$ หรือ PM_{10} ซึ่งอาจซึมลงไปในปอดและส่งผลกระทบต่อสุขภาพ เช่น โรคทางเดินหายใจและโรคหัวใจ นอกจากนี้ การระบาดของโรค COVID-19 ทำให้เกิดความจำเป็นต้องสวมหน้ากากเพื่อป้องกันการแพร่เชื้อไวรัส อย่างไรก็ตาม ไม่ใช่หน้ากากทั้งหมดที่มีคุณสมบัติที่เหมาะสมต่อการป้องกันมลพิษทางอากาศและเชื้อไวรัส ทำให้การเลือกใช้หน้ากากที่เหมาะสมเป็นสิ่งสำคัญในการป้องกันไม่ให้เกิดอันตรายต่อสุขภาพ งานวิจัยนี้มุ่งเป้าหมายที่จะศึกษาผลของการทอของผ้ากรองที่มีตัวทอผ่านการจำลองด้วยการใช้ Computational Fluid Dynamics (CFD) ในการทำการทดลองโดยใช้ระบบเป็นการไหลแบบราบเรียบ (laminar flow) เนื่องจากเรย์โนลด์สเบอร์ของการหายใจมีค่อนข้างต่ำ โดยในการทดลองนี้จะศึกษาไปที่อนุภาคที่มีขนาดเล็กกว่า 10 ไมครอนและศึกษาผลของรูปแบบการทอทั้งสามแบบคือ แบบธรรมดา แบบทแยงและแบบซาติน การทดลองนี้จะใช้การออกแบบโมเดลร่วมกับ Discrete Phase Model (DPM) ในโปรแกรม FLUENT ในการจำลองการไหลของอากาศผ่านผ้ากรองทั้งสามชนิด ในการตรวจสอบความถูกต้องของโมเดลนั้นจะใช้ผลการจำลองเทียบกับข้อมูลของ Konda และเห็นว่าผลของการจำลองนั้นให้ค่าที่แม่นยำในช่วงของอนุภาคระหว่าง 30 - 450 นาโนเมตร ผลลัพธ์ของการวิจัยนี้สามารถนำมาใช้ในการออกแบบหน้ากากที่สามารถป้องกันผู้ใช้จากฝุ่นละอองและไวรัสในขณะที่ออกกำลังกายได้

มหาวิทยาลัย
CHULALONGKORN UNIVERSITY

สาขาวิชา วิศวกรรมเคมี
ปีการศึกษา 2565

ลายมือชื่อนิสิต
ลายมือชื่อ อ.ที่ปรึกษาหลัก

6372108521 : MAJOR CHEMICAL ENGINEERING

KEYWORD: COVID-19, CFD, Cloth masks, Weave pattern, Aerosols, Filtration efficiency

Wisit Bandasak : The Study of Weave-Pattern Effect on Filtration Performance of Woven Filter Cloths by Computational Fluid Dynamic Modeling. Advisor: Asst. Prof. PIMPORN PONPESH, Ph.D.

An important global problem that has an impact on both human health and the environment is air pollution. Exercise and outdoor activities are essential for human well-being, but they can also have a detrimental effect on health and the environment. For example, $PM_{2.5}$ and PM_{10} particles can enter the lungs and cause respiratory and cardiovascular disorders. Moreover, masks must be worn in order to stop the COVID-19 epidemic from spreading. Nevertheless, not all masks are effective in preventing viruses and air pollution. Consequently, selecting the proper mask is essential for avoiding health risks. Using the use of computational fluid dynamics, this study will examine the filtering capabilities of three different types of woven filter materials, including plain, oblique, and satin weaves. The experiment makes use of a laminar flow system and concentrates on particles smaller than 10 microns. The findings demonstrate that the simulation model's predictions for particles with diameters between 30 and 450 nanometers are correct, which may be used to create efficient masks that can shield users from airborne viruses and contaminants as they exercise.

จุฬาลงกรณ์มหาวิทยาลัย
CHULALONGKORN UNIVERSITY

Field of Study: Chemical Engineering

Student's Signature

Academic Year: 2022

Advisor's Signature

ACKNOWLEDGEMENTS

The authors gratefully acknowledge the support provided by the Metallurgy and Materials Science Research Institute (MMRI), Chulalongkorn University, which was instrumental in conducting this research. In addition, I would like to convey our profound appreciation to Dr. Pimporn Ponpesh for her essential support and direction during the execution of this thesis. Her in-depth knowledge of the subject and experience were crucial in determining the course of the study and providing valuable insights. I appreciate your effort and steadfast support.

Wisit Bandasak



TABLE OF CONTENTS

	Page
ABSTRACT (THAI).....	iii
ABSTRACT (ENGLISH).....	iv
ACKNOWLEDGEMENTS	v
TABLE OF CONTENTS	vi
LIST OF TABLES	ix
LIST OF FIGURES	x
CHAPTER 1 INTRODUCTION	1
1.1 Background	1
1.2 Objective	3
1.3 Scope of research	3
1.4 Significant of the study	4
CHAPTER 2 Theory and literature reviews.....	5
2.1 Theory.....	5
2.1.1 Types of woven filter cloths.....	6
2.1.2 Filtration mechanism	9
2.1.3 Theoretical framework for filter cloth design challenges and importance of filtration performance.....	13
2.1.4 Particulate matters	14
2.1.5 Type of masks.....	15
2.1.6 Type of fabric for face masks	17
2.1.7 The Barrier Face Covering Standard.....	18

2.2 Literature reviews.....	20
CHAPTER 3 Methodology	24
3.1 Design scope	24
3.2 Model generating.....	25
3.2.1 Simulation setup.....	27
3.3 Computational fluid domain	28
3.4 Mesh.....	30
3.4.1 Mesh independent test.....	32
3.5 Gas phase model	32
3.5.1 Mass conservation equation.....	33
3.5.2 Momentum conservation equation	33
3.6 Discrete phase model	33
3.7 Analytical model	35
3.7.1 Pressure drop.....	35
3.7.2 Filtration efficiency	36
3.8 Boundary condition	39
3.8.1 Limitation of this work.....	40
3.9 Investigation of weave-patterns effect on filtration performance	41
CHAPTER 4 Results and discussion	42
4.1 Model validation	42
4.1.1 Pressure drop.....	43
4.1.2 Filtration efficiency	44
4.2 Flow field distribution	46
4.3 Influence of filtration velocity	52

4.4 Influence of weave-pattern.....	61
4.5 Quality factor	65
CHAPTER 5 Conclusion.....	67
CHAPTER 6 Recommendation.....	69
REFERENCES	71
VITA.....	77



LIST OF TABLES

	Page
Table 2.1 The advantages and disadvantages of each pattern	9
Table 2.2 The ASTM F3502 standard.....	19
Table 3.1 Properties of material in FLUENT	25
Table 3.2 The parameters used to generate fiber geometry 80 TPI.....	27
Table 3.3 Parameter setting of grids.....	30



LIST OF FIGURES

	Page
Figure 2.1 Observing weaves.....	6
Figure 2.2 Plain weave.....	7
Figure 2.3 Twill weave.....	8
Figure 2.4 Satin weave.....	8
Figure 2.5 Air filtration mechanisms Inertial impaction, Brownian diffusion, Interception, Gravitational effect, and Electrostatic attraction.....	10
Figure 2.6 Theoretical collection efficiencies of aerosol particle collection mechanisms.....	12
Figure 2.7 Particulate matters size comparisons for PM _{2.5} , PM ₁₀ , Human hair and Fine beach sand.....	14
Figure 2.8 Type of masks from <i>CDC.gov</i>	16
Figure 2.9 Comparison chart of single filter efficiency of each material.....	17
Figure 3.1 Peirce geometric model of woven fabric.....	26
Figure 3.2 The plain weave model in this simulation has a warp and weft diameter of 0.27 mm, a distance between the warp cover and the weft of 0.642 mm, and a contact angle of 29.205 degrees.....	28
Figure 3.3 Simulation domain and boundary conditions (SVF = 27.16%, d _f = 270 μm).	29
Figure 3.4 Tetrahedral mesh of the model with max size of element is 0.08 mm and Body of influence size 0.04 mm.....	31
Figure 3.5 The effect of computational domain size on pressure drops.: Total number of elements compare to the pressure drop.....	31

Figure 3.6 A comparison based on analytical model between the three capture mechanisms of Brownian diffusion, interception, and inertial impaction (Plain weave, $d_f = 270 \mu\text{m}$, SVF = 27.16%).	37
Figure 3.7 A comparison based on analytical model between the three capture mechanisms of Brownian diffusion, interception, and inertial impaction (Plain weave, $d_f = 65 \mu\text{m}$, SVF = 27.16%).	38
Figure 3.8 Simulation domains: a) twill weave, b) satin weave Both weaves have the same parameters as plain weave.	41
Figure 3.9 Model of twill weave (left) and satin weave (right).	42
Figure 4.1 pressure drop comparing the experiment and simulation (plain weave model with 0.065 mm diameter and 300 TPI).	44
Figure 4.2 The simulation results of filtration efficiency at flow rate 1.2 CFM with the same plain weave, TPI, fiber diameter, and aerosol type as Konda's research are compared.	45
Figure 4.3 Flow field of fibrous media with different filtration velocity (Plain weave 300 TPI SVF = 27.16%, $d_f = 65 \mu\text{m}$).	47
Figure 4.4 Flow field of fibrous media with different filtration velocity (Satin weave 300 TPI SVF = 27.16%, $d_f = 65 \mu\text{m}$).	48
Figure 4.5 Flow field of fibrous media with different filtration velocity (Twill weave 300 TPI SVF = 27.16%, $d_f = 65 \mu\text{m}$).	49
Figure 4.6 Velocity contour at 0.05 m/s for plain weave on the left, satin weave on the center, and twill weave on the right.	50
Figure 4.7 Velocity contour at 0.18 m/s for plain weave on the left, satin weave on the center, and twill weave on the right.	50
Figure 4.8 Velocity contour at 0.27 m/s for plain weave on the left, satin weave on the center, and twill weave on the right.	51

Figure 4.9 Velocity contour at 0.75 m/s for plain weave on the left, satin weave on the center, and twill weave on the right.....	51
Figure 4.10 Filtration efficiency of particles ranging from 10 to 10000 nm at various filtration velocities (from rest to maximum exertion) from three 300 TPI weaves: a) plain weave, b) satin weave, and c) twill weave	54
Figure 4.11 Filtration efficiency of particles ranging from 10 to 10000 nm at various filtration velocities (from rest to maximum exertion) from three 80 TPI weaves: a) plain weave, b) satin weave, and c) twill weave	56
Figure 4.12 Filtration efficiency of submicron particles (a) and micron particles (b) under different filtration velocities (from rest to maximum exertion) in the plain weave 300 TPI model.....	57
Figure 4.13 Filtration efficiency of submicron particles (a) and micron particles (b) under different filtration velocities (from rest to maximum exertion) in the satin weave 300 TPI model.....	59
Figure 4.14 Filtration efficiency of submicron particles (a) and micron particles (b) under different filtration velocities (from rest to maximum exertion) in the twill weave 300 TPI model.....	60
Figure 4.15 Filtration efficiency for plain, satin, and twill weaves with 300 TPI at varied filtration velocity rates:(a) 0.05 m/s and (b) 0.18 m/s.....	61
Figure 4.16 Filtration efficiency for plain, satin, and twill weaves with 300 TPI at varied filtration velocity rates:(a) 0.27 m/s and (b) 0.75 m/s.....	62
Figure 4.17 Filtration efficiency for plain, satin, and twill weaves with 80 TPI at varied filtration velocity rates:(a) 0.05 m/s and (b) 0.18 m/s.....	64
Figure 4.18 Filtration efficiency for plain, satin, and twill weaves with 80 TPI at varied filtration velocity rates:(c) 0.27 m/s and (d) 0.75 m/s.....	65
Figure 4.19 Quality factor variation with the filtration velocity	66

CHAPTER 1

INTRODUCTION

1.1 Background

Air pollution has long been a serious problem in many parts of the world, harming the environment and the health of millions of people. Particulate matter (PM) is the major cause of air pollution, which is composed of tiny dust, soot, and other pollutants that may be absorbed and cause a range of health problems. $PM_{2.5}$ and PM_{10} are the most researched and controlled. $PM_{2.5}$ particles are those with a diameter of less than 2.5 micrometers and the ability to enter the lungs profoundly [1]. They are frequently released by machines, factories, and wildfires, among other sources, and are linked to several health issues, including lung cancer, heart disease, and stroke. On the other hand, PM_{10} particles, which have a diameter of 10 micrometers or less, can also injure the lungs when inhaled. They are frequently released by sources including building sites, dirt roads, and other dust sources.

For many years now, Thailand has been experiencing problems with dust caused by $PM_{2.5}$ that has been continuously increasing. due to the growth of the city and industry. In addition, increased traffic leads to poor air quality in cities throughout Thailand [2]. The difficulty is worse throughout the winter. When the air temperature is still cooler, the growing use of biomass fuels for cooking and heating has aggravated the situation. Air pollution has a significant negative impact on public health. This results in a higher frequency of respiratory disease as well as increased rates of cardiovascular disease and other disorders [3].

Concerns about PM pollution have grown because of the continuing COVID-19 epidemic since evidence shows that exposure to PM may enhance the chance of getting the virus [4]. PM and air pollution might be particularly concerning for people who like exercising outdoors. It may be challenging to breathe when exercising due to the worsening of respiratory conditions and decreased lung function caused by exposure to these pollutants. Additionally, environmental elements like severe weather might put outdoor exercisers at danger. Since wearing a mask can help guard against the negative

effects of air pollution and lower the danger of catching or transmitting COVID-19, many health professionals advise doing so when exercising outside. However, it's necessary to remember that not all masks are equally efficient, and for the best level of protection, a suitable fit and adequate filtration are essential. Masks may be produced from three different types of materials: woven fabrics, non-woven fabrics, and knitted fabrics. Weaving machinery for weaving wefts and wefts perpendicularly against one other. Non-woven textiles are those that are formed by processes other than weaving, such as film forming, direct injection, or fabric formation from fibers. The last kind, stretch fabric, is created by knitting into a loop of thread so that it interferes with the weft and horizontal lines that are interlaced back and forth. Non-woven textiles give the finest dust filtering due to the narrow space between the threads.

There are several varieties of woven textiles in weaving. The pattern in weaving is the repeated pattern of the fundamental design. Plain, Twill, and Satin weave patterns are the most prevalent. Each design is further segmented. Each of them gives a different gap size and hence a variable filtering efficiency. Different weaving patterns provide varying degrees of strength and flexibility, as well as varying degrees of fabric attractiveness. Furthermore, the kind of fabric, such as Cotton, Chiffon (Chiffon), or Silk (Silk), used to manufacture woven fabrics, impacts the filtering since the threads employed are woven with varying density. As a result, there is a variation in air permeability, and there are also non-woven textiles that may be created from polymers.

Nowadays, besides the problem of air pollution, there is still a problem with COVID-19, a disease caused by the coronavirus. It can be spread by contact with breathing, talking, coughing, and sneezing through droplets. Therefore, it is imperative to wear a mask when leaving the house to prevent infection and to wear it when leaving the house to exercise too. Wearing a non-woven mask may provide greater filtration efficiency but will also make it difficult to breathe during exercise. So, wearing a cloth mask might be a better fit for exercising. Besides air pollution, there is also the problem of COVID-19 disease, which is caused by the coronavirus. It is spread through droplets from breathing, talking, coughing, and sneezing [5]. To avoid infection, it is vital to wear a mask when leaving the house and also when exercising outside. Wearing a non-woven mask may improve filtering

effectiveness, but it will also make it difficult to breathe during activity. Wearing a cotton mask while exercising can be a better option.

The purpose of this study is to use the CFD approach and the FLUENT software to examine the impact of various weave patterns on the filtering effectiveness of masks. The goal of the study is to comprehend the connection between mask design and the efficiency of filtering PM particles. This research can offer insights into the ideal design of masks for use in reducing the negative effects of PM pollution and halting the transmission of COVID-19 and other airborne diseases by analyzing the filtration effectiveness of masks made with various weave patterns using these potent computational tools. To improve the production of cloth masks suitable for exercise.

1.2 Objective

This study intends to address the present dust and coronavirus concerns by investigating the best weaving pattern for filtering dust and viruses during daily activities, including exercise. Because wearing a mask while exercising can make breathing difficult, the goal is to increase filtration effectiveness and design masks that are more acceptable for athletes who must wear masks while exercising. The research entails studying and analyzing the filtration efficiency of various woven fabrics in filtering through such fabrics using computational fluid dynamics, as well as investigating the appropriate fabric patterns for filtering particles smaller than PM_{10} to improve the design of exercise masks.

1.3 Scope of research

This research studied the filtration efficiency of various woven fabrics using Computational Fluid Dynamics (CFD) to improve the design of small-particle filtering masks for exercising. The scope of the research includes the following:

- 1.The model simulation is of yarns made of silk with three weaving patterns, including plain, twill, and satin.
- 2.The inlet velocity of air flowing through the model between 0.05 to 0.75 meters/second.
- 3.The particle size used in the experiment was smaller than 10 microns.

1.4 Significant of the study

This research can be utilized to develop excellent dust-reduction filters. viral and comfortable to wear when exercising in order to produce a more appropriate mask and understand the behavior of particles moving in the air via various types of masks to determine how many particles can pass through. Which format is most appropriate by applying fluid dynamics calculations and a simulation tool to assist lower the real expense of doing direct experiments.



CHAPTER 2

Theory and literature reviews

In this chapter, information and theories related to this research are discussed. as well as other research related to filtering and computational fluid dynamics data to help conduct the experiment will be given in this chapter.

2.1 Theory

Filtration is a critical step in many industries. pollution control, food and beverage production, medicines, and oil and gas Filtration is used to remove undesired particles such as particles, contaminants, and pollutants from liquids or gases. Woven filter cloths are frequently employed as the filtering medium in a variety of filters, including bag filters, press filters, and push filters to accomplish this aim. Fibers are woven together in a precise pattern to generate a porous structure in these filter cloths with a variety of pores of varying sizes and locations. Many factors influence the effectiveness of this filtration process. includes the fiber type and the weaving style. That is why knowing the function and performance of filter media is critical in a variety of circumstances. To obtain maximum filtration while maintaining product quality in a variety of sectors.

Woven filter cloths have been used to filter liquids and gases in various ways for ages. Thailand has used woven filter cloth since ancient times. It is used to filter the liquid and oil in the lamp. Most of these woven filter cloths are composed of natural fibers like cotton, wool, or silk. Since the early twentieth century, woven filter cloths have been employed in face masks [6], although early materials such as cotton gauze were ineffective in filtering particles and were not breathable [7]. Since then, woven filter cloths made of synthetic fibers like polypropylene have been created, which are woven in certain patterns and densities to increase filtering efficiency while retaining breathability. Manufacturing and materials science developments have resulted in ongoing improvements to woven filter cloths used in masks, resulting in more effective and breathable fabrics. N95 respirators

give the maximum level of protection but are not always required, and fabric masks and surgical masks can be useful if correctly used and have adequate filtering efficiency and breathability [8].

2.1.1 Types of woven filter cloths

The three main weave styles utilized in woven filter cloths are satin, twill, and plain weaves. Each pattern has different properties, advantages, and disadvantages. [9, 10]: When weaving, different techniques for interlacing fibers are used. The procedure involves a vertical line called the warp line and a horizontal line known as the weft line. Each square on the fabric corresponds to the intersection of these two lines. These lines can intersect in two ways: the vertical line can overlap the horizontal line, or the horizontal line can only overlap the weft line. When the horizontal line goes beyond the weft line, a black square is used to represent it, while a white square is used when the weft line overlaps the horizontal line. Figure 2.1 illustrates this.

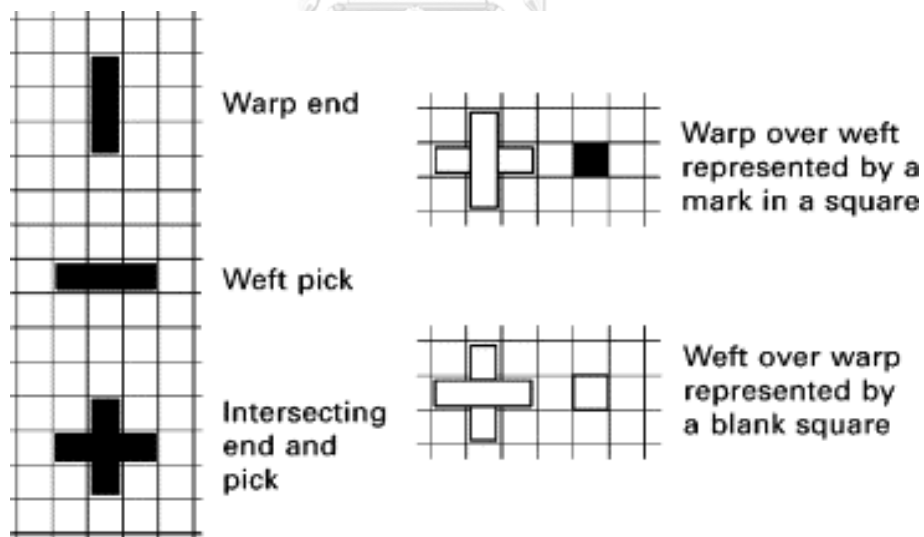


Figure 2.1 Observing weaves.[11]

Plain weave: Plain weave is the most basic and fundamental weave used in woven filter cloths. It is woven on a 2-harness loom with threads at right angles, with each warp yarn interlacing with each weft yarn. Unless there is a surface design, this produces a square

and uniform weave pattern that is reversible. Plain weave cloths are the least expensive to make, firm, and long-lasting, but they wrinkle more and are less absorbent. They are very resistant to abrasion and are frequently used as a background for printing or embroidery. Plain weave cloths, on the other hand, have low filtering efficacy due to their larger pore size, which enables some particles to get through. Balanced plain weaves, where the warp and weft are made of threads of the same weight, and basket weaves, where two or more threads are grouped and then woven, are also types of plain weave. The plain weave is shown in Figure 2.2.

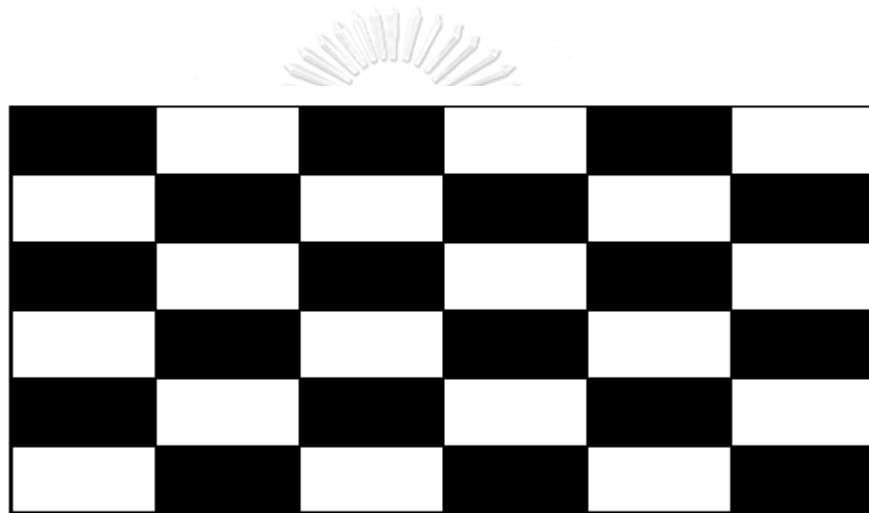


Figure 2.2 Plain weave

จุฬาลงกรณ์มหาวิทยาลัย

CHULALONGKORN UNIVERSITY

Twill Weave: The diagonal pattern in this weave is achieved by passing the weft threads over and under many warp strands before going on to the next row. This weave is denser than plain weave and has fewer pores, resulting in improved filtering effectiveness. The diagonal design also increases the fabric's flexibility and makes it less prone to ripping. Twill weave fabrics, on the other hand, are less consistent and have a coarser surface roughness. The twill weave is shown in Figure 2.3.

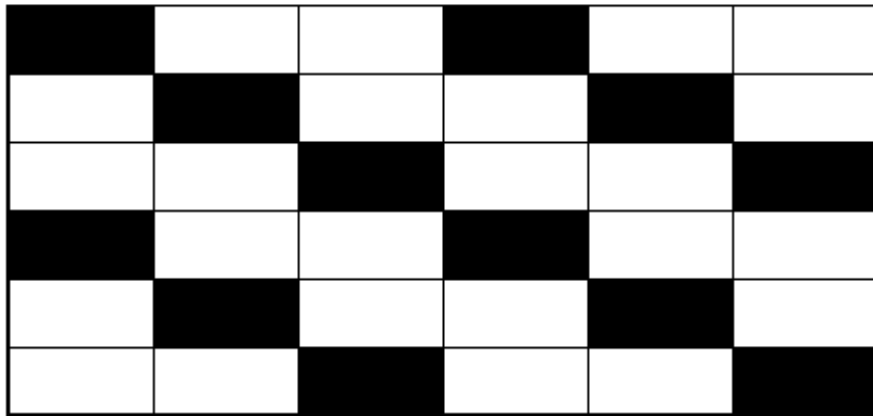


Figure 2.3 Twill weave

Satin Weave: The satin weave is a style of cloth weaving recognized for its shiny look, created by combining threads with equal shine. This weaving structure is made up of four or more weft or fill threads floating over a warp yarn, or four warp yarns floating over a single weft yarn. Satin weave fabrics feature a smooth, shiny surface and fewer interlacing points than plain or twill weave fabrics, resulting in a much finer, smoother material with a tighter weave and smaller pore size. This makes them suitable for applications needing high particle removal levels, such as pharmaceutical or semiconductor production, but their smooth surface texture can make them more prone to clogging and more difficult to clean. The satin weave is shown in Figure 2.4.

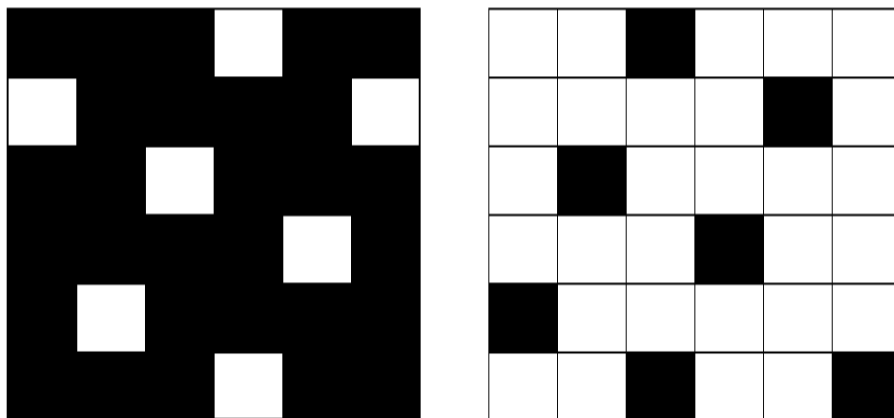


Figure 2.4 Satin weave

Table 2.1 The advantages and disadvantages of each pattern[12]

Weave Type	Advantages	Disadvantages
Plain Weave	Easy to produce; strong and durable	Not as flexible as other weaves; not suitable for intricate designs; may have limited airflow
Twill Weave	Provides a diagonal pattern that can hide stains and wear; more pliable than plain weave; more durable than other weaves	Production can be more expensive than plain woven fabrics; may be less breathable than conventional woven fabrics; may have less airflow than other woven fabrics
Satin Weave	Has a shiny and smooth appearance; highly flexible and durable; can be produced with high thread counts	Can be expensive to produce; may be less durable than other woven fabrics; may not be suitable for high tensile applications

2.1.2 Filtration mechanism[13, 14]

The removal of airborne particles from the air via a filter is a critical operation in the air filtering system. This process depends on several types of physical and chemical mechanisms like interception, impaction, diffusion, electrostatic attraction, adsorption, and gravitational to ensure that the air is free of pollutants. The efficacy of the filtering process is determined by elements such as particle size and characteristics, filter design and materials, and application. All filtration mechanisms are shown in Figure 2.5.

Inertial impaction: Inertial impaction is a filtering technique in which bigger particles in the air are unable to follow the airstream around filter fibers due to their size and instead crash with the fibers and become stuck. This technique works best when the gas velocity is high, and the filter material is densely packed with fibers. Inertial impaction is very effective for particles bigger than 1 micron in size. The efficacy of the above steps depends on the size and shape of the filter fibers, the air flow velocity, and the size and density of the particles being filtered.

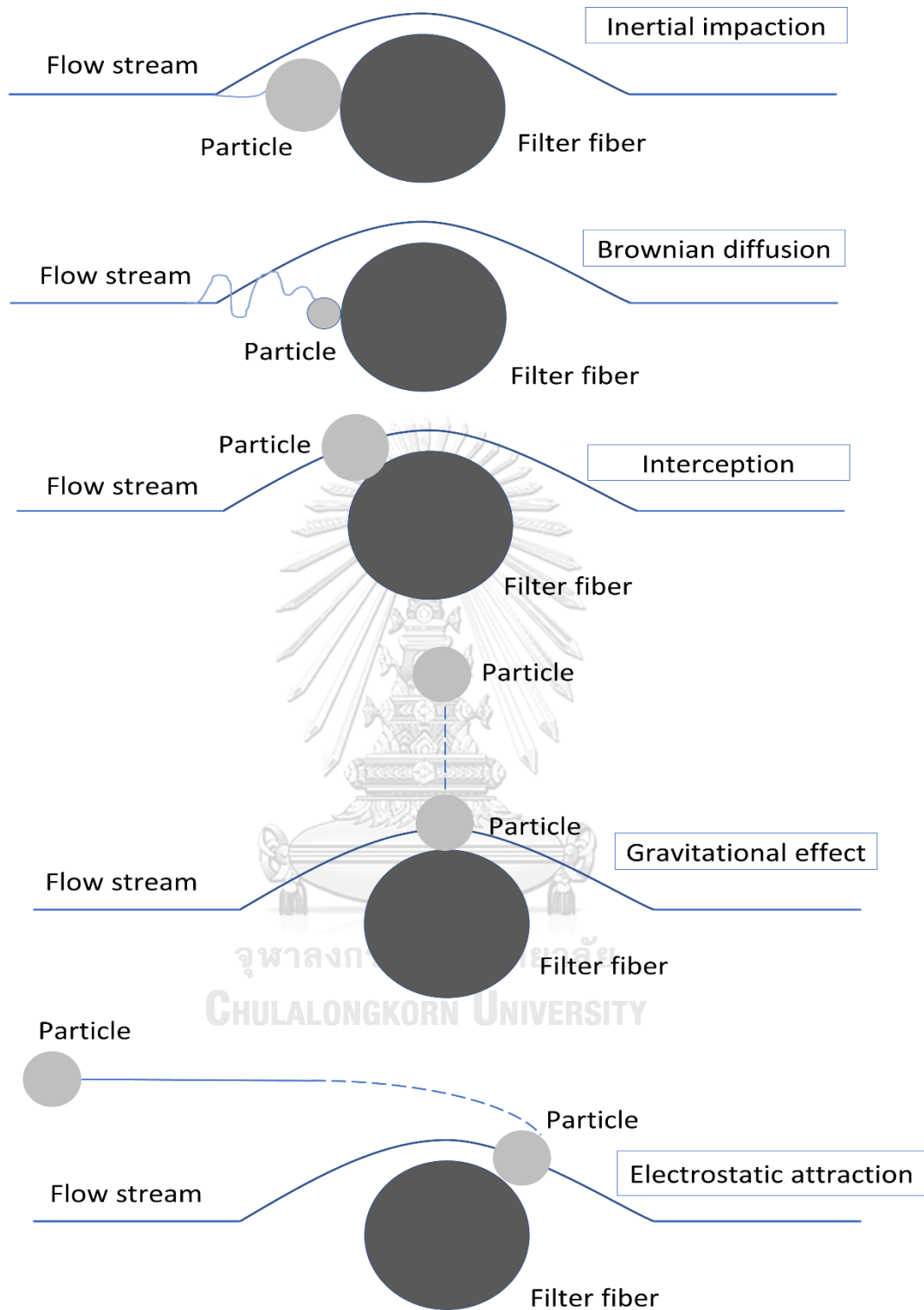


Figure 2.5 Air filtration mechanisms Inertial impaction, Brownian diffusion, Interception, Gravitational effect, and Electrostatic attraction.

Diffusion: When particles are transported by air currents and collide with gas molecules in the air, diffusion is a filtering process that is efficient for ultrafine particles less than 0.1 micron. Examples of particles in this size range include small aerosols and fine dust, and viruses. These particles will reverse direction and become entangled on the surface of the filter fibers. Many factors influence diffusion efficiency, including the size and arrangement of the filter fibers. The efficiency of the Brownian effect is reduced for particles with a diameter greater than 0.3 micron [15] because these particles do not deviate from the streamline and can only be collected on the fiber surface through this mechanism. The airflow rate and airborne particle concentration are factors that can influence the efficiency of this process. Diffusion may be a powerful filtering process.

Interception: The interception mechanism is a filtering process that happens when big particles collide with the filter fibers as air travels through the filter. The fiber itself captures particles larger than the gap between the fibers. The size and form of the filter web, the speed of air movement, and the size and density of the particles being filtered all influence interception efficiency. This technique is especially efficient for particles approximately 1 micron (1000 nanometers) and larger. The size of these particles could range from dust and pollen (approximately 10 microns) to bacteria (1-10 microns) and even some large viruses. When particles approach the filter fiber at an angle, larger particles collide with the fibers, while smaller particles are blown through the fibers and are not captured.

Electrostatic effect: The electrostatic effect in filtration occurs when charges exist on both fibers and particles, causing them to attract each other. However, in most cases, the induced electric field and resulting attractive force from these charges are very weak and can be neglected. Therefore, intentional charging of filter fibers with a static charge is often used to enhance the electrostatic attraction mechanism in filtration. This mechanism is effective in capturing both small and large particles, including ultrafine particles smaller than 0.1 micron. Their efficiency depends on the size and distribution of the electrostatic charge, the shape and size of the filter fibers, and the concentration of charged particles in the air. Electrostatic attraction is often combined with other filtration mechanisms for optimal particle capture.

Adsorption: Adsorption filtration is a process that involves the removal of contaminants from fluids or air by adsorbing them onto a filter medium. The adsorption mechanism is driven by surface forces such as van der Waals forces, electrostatic interactions, and chemical bonding. Adsorption filtration is a well-known technique for removing pollutants from fluids and air that is employed in plenty of industrial, environmental, and health-related applications. The filter medium needs to be replaced or regenerated periodically to restore its adsorption capacity. Overall, adsorption filtration plays a critical role in improving the quality of fluids and air and promoting a healthier and safer environment.

Gravitational effect: Gravitational effect filtering is a mechanism by which particles deviate from the streamline and accumulate on the fiber surface due to the influence of gravity as they pass through the fiber layer. However, this mechanism is ineffective for particles smaller than 0.5 microns in diameter, as the particles pass through the fiber layer without accumulating on the fiber surface. Due to the short airflow through the fiber air filter, especially filter paper. Therefore, the effect of gravitational accumulation can be ignored.

The effectiveness of each of these mechanisms depends on various factors, including fiber size and shape, speed of air flow, and the concentration and size of the filtered particles. Combinations of these mechanisms are commonly used in woven filter cloths to achieve the desired level of filtration efficiency.

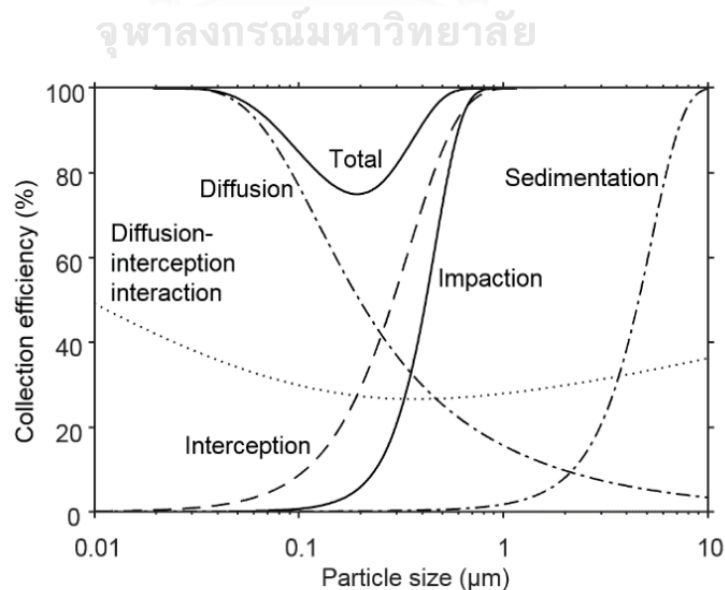


Figure 2.6 Theoretical collection efficiencies of aerosol particle collection mechanisms [16]

2.1.3 Theoretical framework for filter cloth design challenges and importance of filtration performance.

Filtration performance is critical in the design and manufacture of masks, particularly in the event of a pandemic. It is critical that the mask's filter captures and prevents the transmission of airborne particles such as viruses and bacteria. A high-quality filter can lessen transmission risk and protect both the wearer and others around them. Inadequate filtering might provide a false impression of security and expose persons. As a result, filtration performance must be prioritized in mask manufacture to ensure their efficiency in avoiding the spread of infectious illnesses. When analyzing a mask's filtration performance, net filtration efficiency (NFE) is an essential measure to examine. NFE is a measure of a mask's ability to filter out particles of a specific size, typically measured at the most penetrating particle size (MPPS), which is the particle size at which the filter has the lowest efficiency. In the case of MPPS masks, MPPS is generally between 0.1 and 0.3 microns for aerosols and respiratory droplets. A mask's NFE at the MPPS is an important factor in determining its effectiveness in filtering out potentially harmful particles. Generally, masks with higher NFE values at the MPPS are more effective at filtering out particles, providing better protection for the wearer. Therefore, NFE at the MPPS is a critical parameter to consider when evaluating the filtration performance of masks for various applications. The graph about NET or collection efficiency is shown in Figure 2.6.

Designing woven filter cloths presents various issues that must be addressed to provide optimal performance. One of the most difficult difficulties is balancing filtering efficiency with pressure decrease. Increasing weave density and decreasing pore size can enhance filtration efficiency but also increase pressure drop, making it more difficult for air or liquid to pass through the filter. This trade-off must be carefully considered to ensure that the filter captures the desired particles without causing excessive pressure decrease.

Computational fluid dynamics (CFD) simulation is a powerful tool for investigating the filtration performance of woven filter cloths, especially in terms of studying different weave patterns. With CFD, it is possible to visualize the flow of fluid through a filter cloth and to calculate important parameters such as pressure drop and filtration efficiency. By varying the weave pattern and other parameters, designers can optimize the performance of woven filter cloths for specific applications. However, CFD simulation has limits since

the accuracy of the findings is heavily reliant on the assumptions made and the quality of the input data. Therefore, CFD should be used in conjunction with experimental testing to validate the results and ensure that the designed filter cloths meet the required specifications.

2.1.4 Particulate matters

Particulate matter (PM) is combination of microscopic particles that might be natural or man-made in origin. Natural sources consist of dust and particles, while man-made ones include emissions from vehicles, factories, and power plants. PM can be categorized based on particle size, with the tiniest particles providing the highest risk to human health. PM_{10} refers to particles with a diameter of 10 micrometers or less, while $PM_{2.5}$ refers to particles with a diameter of 2.5 micrometers or less [17]. Particulate matter (PM) released into the air stays in the air for a long time and is carried by the wind. From respiratory irritation to more serious conditions such as heart disease and lung cancer. With the outbreak of COVID-19, wearing a face mask has become an important protection against the virus. And masks with high filtration efficiency are especially important in areas with high PM pollution.

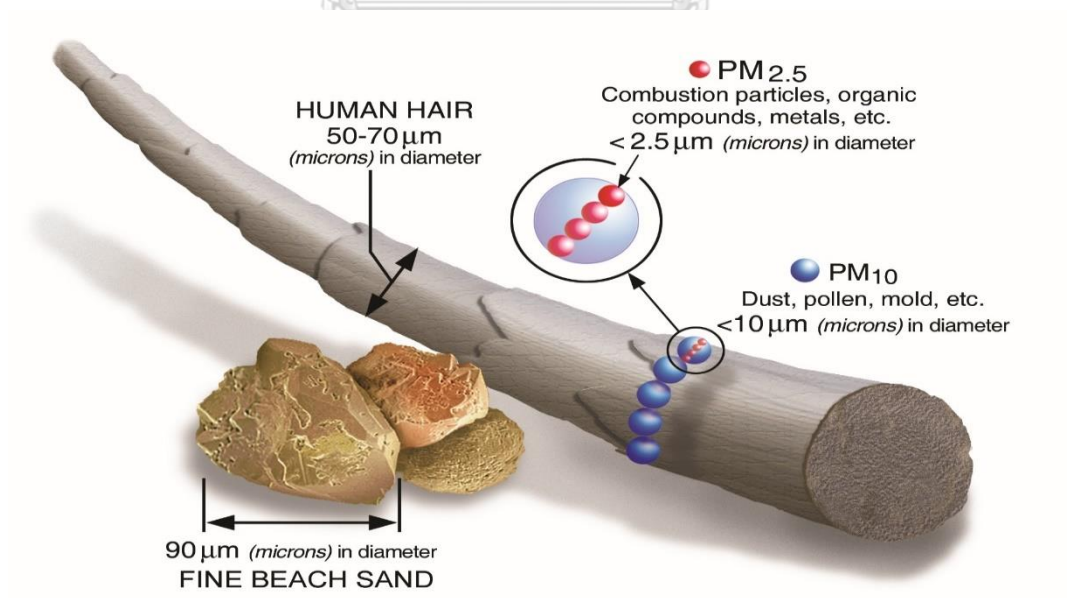


Figure 2.7 Particulate matters size comparisons for $PM_{2.5}$, PM_{10} , Human hair and Fine beach sand[18]

2.1.5 Type of masks

Masks come in lots of types and are frequently used for a choice of purposes, including respirator mask, Face mask and cloth mask within each category. There may be differences in design and filter performance. Mask standards come in many places: ASTM, NIOSH, and EN are three different organizations that produce standards and guidelines relevant to different industries, including health care, work safety and environmental protection. ASTM International [19] is a globally recognized organization that develops and publishes technical standards for a wide range of materials, products, systems, and services. Their standards cover a wide range of industries, including healthcare, construction, and manufacturing. NIOSH (National Institute for Occupational Safety and Health) [20] is a government agency founded in the United States that sets standards for respirators, including masks. NIOSH-approved masks have been thoroughly evaluated for their ability to filter airborne pollutants. EN (European Norm) is a set of standards developed by the European Committee for Standardization (CEN) for various industries, including medical devices. EN standards are used to ensure the safety and efficacy of products and services within the European Union. Each organization has its own set of standards and guidelines. But they all aim to promote safety, quality, and efficiency across industries. These standards are frequently updated and revised to keep up with new technologies, research, and best practices.

Respirator masks are intended to keep the wearer from inhaling potentially dangerous chemicals such as airborne particles and gases. These masks often feature a tight fit and use advanced filtration materials to catch particles, such as electrostatically charged fibers or activated carbon. They are frequently employed in industrial settings where workers are exposed to potentially dangerous products.

Surgical masks, on the other hand, are designed to keep patients and others' respiratory emissions at bay. These masks commonly consist of polypropylene or cellulose and are intended to be worn loosely, frequently used in hospitals to prevent the spread of infectious illnesses.

Cloth masks are a type of face mask made of cotton, silk, or synthetic fibers. It is usually reusable and when cleaned it can be reinserted. Although cloth face masks may not provide the same level of protection as respirators or surgical masks, they do provide

protection. However, these masks are effective in reducing respiratory aerosol transmission and are more desirable to use for longer periods of time. Because of their diverse physical qualities, different kinds of fibers have varying filtering performance. resulting in power Cotton fibers with a count of 600 threads, that is, 300 threads in the weft and 300 threads per square inch, have a filtering efficiency of up to 79 % for particles smaller than 300 nm and up to 98.4% for particles larger than 300 nm when compared to fabrics made from other similarly woven fibers [21]. The better the filtering efficiency, the more layers that overlap.

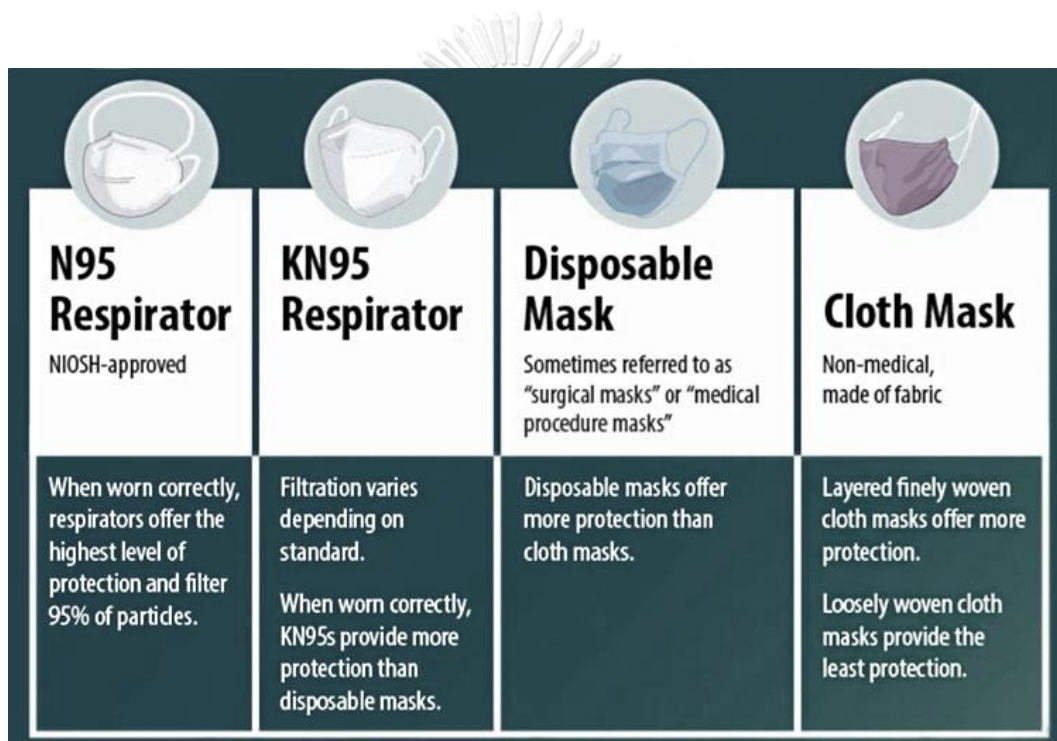


Figure 2.8 Type of masks from *CDC.gov*.

Studies have shown that any type of respirator can filter out smaller particles when exposed to high-velocity air, such as air. coughing or sneezing during high-speed coughing Even N95 masks filter out only 53% of fine particles. Surgical masks filter about 48% less. As shown in Figure 2.9.

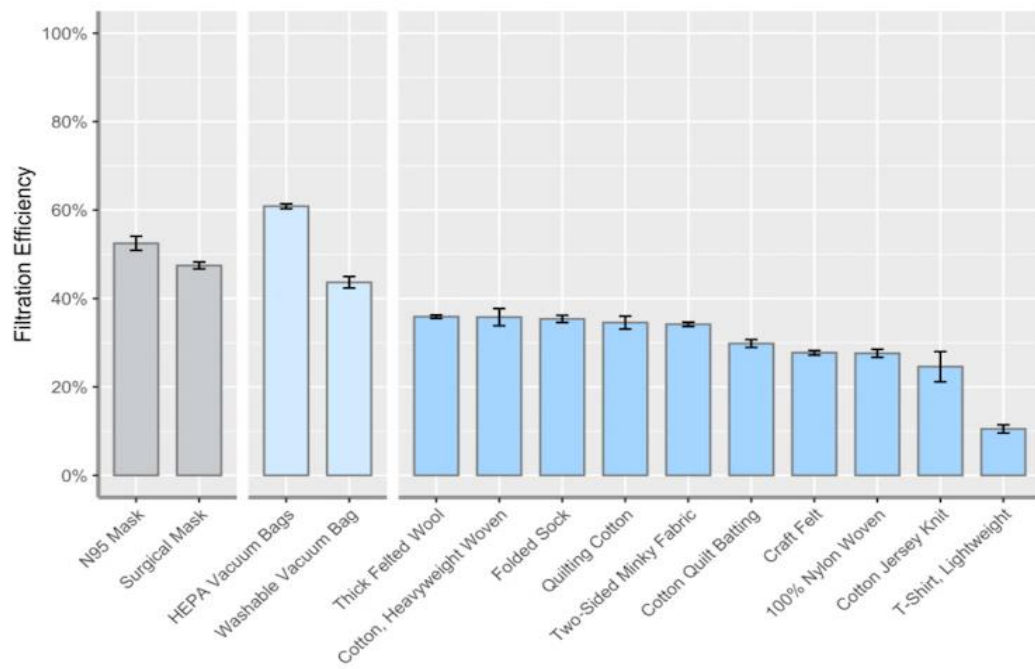


Figure 2.9 Comparison chart of single filter efficiency of each material[22].

As each fabric has different physical properties, it results in different filtration capacities for each fabric type. Most of the fabrics used to make respiratory protection masks are non-woven fabrics because they can be formed without being woven, thus leaving a small gap between the fibers. To have a higher filter efficiency than woven fabrics. But this fabric is not suitable for exercising because of the small gaps that make it very difficult to breathe. Because exercising requires four times more air than resting [23], woven fabrics are more suitable for exercising.

2.1.6 Type of fabric for face masks

Nonwoven fabrics are made by sticking fibers together instead of weaving or knitting. Instead, the fibers are glued together using heat, chemicals, or pressure to form a sheet-like material. Nonwoven fabrics can be made in various methods like Thermal bonding, Hydroentanglement, Needle punching/needle felting and chemical bonding [24]. Nonwoven fabrics are widely used in disposable items such as face masks, cleaning wipes and sanitary pads [25]. As in the construction, filtration, and automotive sectors, nonwoven

materials are cheap and lightweight. But they may not be as durable or breathable as woven or knitted fabrics.

Knitted textiles: Knitted textiles are made by interlacing threads to make a cloth. Knitted textiles are manufactured from a wide range of fibers. Cotton, wool, and synthetic fibers are common fabrics used in apparel, home textiles, and sporting. Knit textiles tend to stretch and stretch. They are lightweight and comfortable to wear. They may not, however, be as robust or durable as woven materials. and may have loose weaves that impact filtering qualities.

Woven Fabrics: Woven fabrics are formed by twisting threads at right angles. Woven fabrics are widely used in apparel, household textiles and industry Made from various fibers such as cotton, wool, silk, and synthetic fibers. The woven fabric is strong and durable. with tight weaves that can provide superior filtering capabilities, however, they may not be as flexible or supple as knitted fabrics.

2.1.7 The Barrier Face Covering Standard

ASTM F3502 is a critical ASTM standard that addresses barrier face coverings, also known as "COVID masks," and was produced in response to the COVID-19 pandemic. It creates a common testing approach to validate the efficacy of these masks as a voluntary standard for mask makers. The standard focuses on four critical parameters: filtration efficiency, airflow resistance, re-use potential, and leakage, giving consumers valuable information to help them make informed purchasing decisions. Many mask packages promise to emphasize the mask material's filtration performance but fail to provide comprehensive information about the overall level of protection provided. ASTM F3502 specifies the basic standards for barrier face covering design, performance, testing, compliance, and labeling. Conformity requirements ensure that products branded "compliant" meet all of the specifications' criteria [26].

Barrier face coverings must adequately cover the wearer's nose and mouth and fit securely to prevent gaps to meet the standard design requirements. They should also have means to maintain the covering in place, such as ties, ear loops, or harnesses. These face coverings can be intended for single use or re-use, and they must be made of non-irritating, non-toxic material that is safe, robust, and able to handle normal handling and

use. They should also be free of sharp edges or points, and they should not include any vents or valves. Overall, ASTM F3502 is critical in ensuring that barrier face coverings meet precise standards for effectiveness, safety, and usability, so increasing consumer confidence and supporting informed decision-making when choosing appropriate masks for personal protection.

To ensure that barrier face coverings provide these functions, ASTM F3502 establishes design and performance criteria in three general areas: 1) protection, 2) comfort, and 3) reusability [27].

ASTM F3502 establishes requirements for masks to guarantee a secure fit that completely covers the mouth and nose. It is necessary to provide sizing information as well as procedures for attaching the masks to the face. The efficacy of filtration varies according to particle size and testing methodologies. The standard adheres to NIOSH recommendations, testing masks against 0.3 μ m particles as a worst-case scenario; however, filtration against bigger particles is often higher. Breathability and filtration testing on completed masks take materials, design, and construction into account.

Furthermore, the standard covers the reusability of barrier face coverings. Laundry instructions must be supplied, and masks must meet fit, filtration, and breathability standards both when new and after the maximum recommended laundering cycles. This guarantees that the masks remain effective and operate well after several uses and cleanings, distinguishing them from single-use medical masks and respirators.

Table 2.2 The ASTM F3502 standard

Face Covering Type	Classification	Performance
Filtration: Sub-micron particulate filtration efficiency (~0.3 μ m)	Level 1	$\geq 20\%$
	Level 2	$\geq 50\%$
Breathability: Air flow resistance	Level 1	≤ 15 mm H ₂ O
	Level 2	≤ 6 mm H ₂ O

Both breathability and filtration can be tested on the same face covering for this new ASTM F3502 standard. To meet the standards for reusable face coverings, a total of 20 masks must be tested: Ten face coverings were evaluated when they were fresh, and ten face coverings were tested after the maximum number of laundering cycles. A face velocity of 10 ± 0.5 cm/sec shall be used. The specimens shall be tested at a flow rate of 85 ± 4 Lpm.

2.2 Literature reviews

Tung et al. (2002) [28] investigation of fluid flow via multifilament woven filter cloths using computational fluid dynamics (CFD). The research shows that the structure of fabric pores has a substantial impact on the flow pattern and downstream resistance, with plain weave exhibiting the highest fluid-flow resistance, and satin weave the lowest, among different woven architectures. These findings suggest the importance of selecting appropriate weaving patterns to improve the filtration efficiency of masks and to facilitate comfortable breathing during physical activities.

Cao et al. (2020) [29] used a semi-analytical model combined with CFD on a Voronoi-based microstructure to examine the filtering performance of fibrous medium. Their study's goal was to increase knowledge of the link between the microstructure of fibrous media and its filtering performance, which is similar to your goal. The fluid flow through the fibrous medium was modeled using a pore-scale filtering mechanism in the semi-analytical model and CFD simulations. The study's findings revealed that the microstructure of fibrous media has a major impact on its filtration performance; particularly, the pore size distribution and pore connectivity were discovered to be critical factors influencing filtration efficiency. It was also discovered that using a Voronoi-based microstructure in CFD simulations proved effective. The study's findings have significant significance for the design and optimization of fibrous media for diverse filtering applications, which is pertinent to your goal of boosting filtration efficiency.

The work "Modeling and CFD-Simulation of Woven Textiles to Determine Permeability and Retention Properties" by Erik Glatt (2011) [30] aimed to utilize computational fluid dynamics (CFD) to model fluid flow through woven textiles and determine their permeability and retention properties. The research involved creating a

virtual model of a woven fabric using ANSYS Fluent software and solving the Navier-Stokes equations for fluid flow. The study demonstrated that CFD simulations can provide an accurate estimation of the permeability and retention properties of woven fabrics. The research also highlighted the significant influence of textile geometry, including porosity, pore size, and yarn diameter, on the flow characteristics. The study also revealed that the weave pattern and yarn arrangement affect the permeability and retention properties of the textile. The findings of the study provide valuable insights into the use of CFD simulations for the analysis of woven textiles, and by understanding the impact of textile geometry and weave pattern on permeability and retention properties, it is possible to optimize textile design for specific applications.

The study by Marc Bénése, Laurence Le Coq and Camille Sollicec (2006) [31] aimed to characterize the filtration performance of a woven filter made of multifiber yarn by experimentally determining its collection efficiency during loading. In this investigation, aerosol particles of known size and concentration were loaded onto the filter, and the collection efficiency was assessed. The results revealed that the collection effectiveness of the filter was influenced by various factors, including particle size, concentration, and the filter's fiber diameter and porosity. The study also developed a two-tier single fiber model to predict the filter's collection efficiency, and the actual and modeled results agreed well. The research provides valuable insights into the filtration performance of woven filters made of multifiber yarn and highlights the use of modeling tools for optimizing filter design. By understanding the factors that influence collection efficiency, filter designers can optimize the filter's fiber diameter and porosity to enhance its performance for specific applications.

Sheldon's (2008) [32] investigated the use of computational fluid dynamics (CFD) to model flow through single layer woven fabrics, specifically wind tunnel screens. The research aimed to determine the accuracy of CFD simulations in reproducing experimental measurements of pressure drops across the screens for Reynolds numbers between 50 and 300. The results showed that CFD simulations were able to accurately predict the pressure drops across the screens. Additionally, the study investigated the impact of variable screen filament spacing on flow rate and found that changes in filament spacing resulted in only a localized change in the flow field. The study's findings have implications

for the design of wind tunnels and paper machine forming fabrics, where the use of CFD simulations can provide accurate predictions of flow behavior and guide the optimization of fabric design.

The work "Direct Numerical Simulation of Cake Formation during Filtration with Woven Fabrics" by David Hund (2018) [33] focused on utilizing direct numerical simulation (DNS) to analyze cake formation during filtration with woven textiles. The researchers simulated the deposition of particles onto a woven fabric surface and the subsequent development of a cake layer. The study's findings revealed that the fabric weave structure, as well as the size and shape of the particles, impact the cake forming process. The cake layer can also change flow patterns and pressure drop throughout the cloth, according to the study. Overall, the work sheds light on the intricate interactions that occur between woven textiles and particles during filtering procedures, which could be helpful in improving the design of woven fabrics for filtering particles in masks for exercise.

The research of Nazarboland (2010) [34] conducted a study on the use of computational fluid dynamics (CFD) to model fluid flow through woven filters and measure their filtering efficiency. The study aimed to create a model that can accurately predict the filtering performance of woven filters based on their structural features. The study found that the developed model was able to reliably estimate the filtration effectiveness of woven filters with varying structural features. Furthermore, the study emphasized the importance of understanding the relationship between the structural features of woven media and its filtering performance. The findings of this study are valuable for the design and improvement of woven filters for specific filtering applications.

All of these studies investigate the filtration performance of woven fabrics using computational fluid dynamics (CFD) simulations. Tung et al. (2002) analyze the impact of different weave patterns on fluid flow resistance and filtration efficiency, while Cao et al. (2020) study the relationship between microstructure and filtration performance. Glatt et al. (2011) focus on the permeability and retention properties of woven textiles, and Benesse et al. (2006) examine the collection efficiency of a woven filter made of multifiber yarn. Green et al. (2008) investigates the flow through single layer woven fabrics, specifically wind tunnel screens, and Hund et al. (2018) analyze cake formation during

filtration with woven textiles. Nazarboland et al. (2010) create a model to predict the filtering effectiveness of woven filters based on their structural features.

The literature review provides a comprehensive overview of current knowledge on airborne particle filtration, highlighting the efficiency of various fabrics and materials in filtering dust and viruses. It emphasizes the need to design masks that are suitable for athletes or individuals engaged in vigorous activities, as conventional masks can impede breathing and cause discomfort. The study aims to develop a mask that is both comfortable and efficient in filtering particles during exercise, with a particular focus on investigating the appropriate fabric patterns for filtering particles smaller than PM_{10} . To achieve this goal, the study will employ computational fluid dynamics to measure the filtration efficiency of different textiles. The COVID-19 pandemic has highlighted the importance of face masks in reducing the spread of respiratory infections, and the study underscores the need for further research to develop reliable masks and air purification systems to protect individuals from pollutants such as dust and viruses.

CHAPTER 3

Methodology

This chapter is divided into 6 parts including design scope, gas phase model, discrete phase model, analytical model, model generating, and mesh independent test.

3.1 Design scope

As noted in the preceding chapter, research from literature uses computational fluid dynamics (CFD) simulations to study the filtration performance of woven textiles. They investigate numerous aspects that influence filtering performance, including weave patterns, microstructure, permeability, retention qualities, collection efficiency, and cake formation. The outcomes of these investigations give important insights into the complicated interactions between woven fabrics and particles during filtering methods. In this project, Utilizing CFD simulations, the filtration effectiveness of different woven textiles will be assessed, aiming to enhance the design of exercise masks. Configuring the conditions of this experiment using the FLUENT software to be appropriate for people's breathing levels during exercises of varying intensity. There are four levels: resting, light exertion, moderate exertion, and maximum exertion. At moderate effort and maximal effort, the speed at which air travels through the mask varies depending on the level. And tested all 3 patterns: plain weave, twill weave, and satin weave, with the values according to the Table 3.1 [35].

Table 3.1 Properties of material in FLUENT

Properties	Value	
Air		
Density	1.2 kg/m ³	
Dynamic viscosity μ	1.8 x 10 ⁻⁵ Pa. s	
Kinematic viscosity ν	1.5 x 10 ⁻⁵ m ² .s ⁻¹	
Cotton		
Density	1500 kg/m ³	
Type of breath	Flow rate	Flow velocity
resting	6 l/min	0.05 m/s
light exertion	20 l/min	0.18 m/s
moderate exertion	30 l/min	0.27 m/s
maximum exertion	85 l/min	0.75 m/s

The flow velocity is calculated from the area and is fully enclosed and the mask area is 190 cm² [36]. This study will focus on the use of computational fluid dynamics (CFD) simulations to investigate the filtration efficiency of various woven fabrics. The study will not include experimental testing of the fabrics. The study will be limited to the filtration of particles smaller than PM₁₀. The study will also be limited to the use of woven fabrics in the design of masks for exercise.'

3.2 Model generating

The model for this study was created by ANSYS Spaceclaim. The first step is to create a fibers model according to Peirce's mathematical model shown in Figure 3.1 [37], offers a mathematical model for combining the factors of the geometrical structure of a plain weave fabric with circular threads. There are some mathematical equations between fabric structural parameters of Peirce's model as follows [37, 38]:

$$h_j + h_w = D_j + D_w = D \quad (1)$$

$$\frac{h_j}{\alpha_w} = \frac{4}{3}\sqrt{c_j}; \frac{h_w}{\alpha_j} = \frac{4}{3}\sqrt{c_w} \quad (2)$$

$$\alpha_w = (l_j - D\theta_j)\cos\theta_j + D\sin\theta_j \quad (3)$$

$$\alpha_j = (l_w - D\theta_w)\cos\theta_w + D\sin\theta_w \quad (4)$$

$$c_j = \frac{L_j}{A} - 1 = \frac{l_j}{\alpha_w} - 1; c_w = \frac{L_w}{B} - 1 = \frac{l_w}{\alpha_j} - 1 \quad (5)$$

$$l_j = \frac{L_j}{N_w}; l_w = \frac{L_w}{N_j} \quad (6)$$

$$\alpha_w = \frac{A}{N_j} = \frac{l_j}{1+c_j} = \frac{L_j}{N_w} \frac{1}{1+c_j} \quad (7)$$

$$\alpha_j = \frac{B}{N_w} = \frac{l_w}{1+c_w} = \frac{L_w}{N_j} \frac{1}{1+c_w} \quad (8)$$

Where α_w and α_j are the spacing between the adjacent weft or warp, c_j and c_w are the warp and weft shrinkage of fabric, h_j and h_w are the crimp wave heights of warp or weft, l_j and l_w are the crimp wave lengths of warp or weft, L_j and L_w are the lengths of warp or weft, N_j and N_w are the numbers of warp or weft, θ_j and θ_w are the contact angles of warp cover on weft or weft cover on warp, A is the length of the fabric, and B is the width of the fabric.

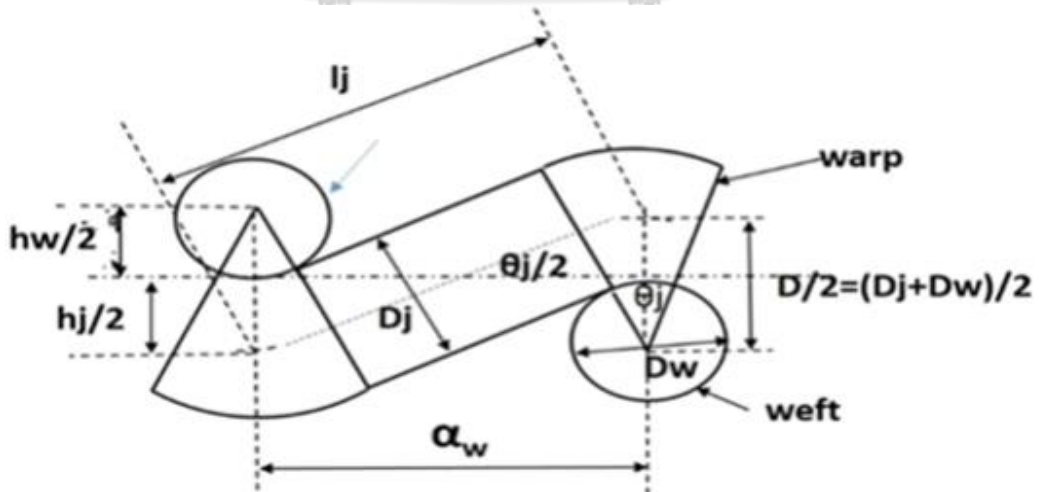


Figure 3.1 Peirce geometric model of woven fabric[38]

If follow the Peirce model for designing, the curved sections of the fibers may exhibit significant skewness. Hence, the objective is to minimize the angle between the fibers, thereby reducing any overlap and achieving a well-aligned model. The fibers that were created were chosen to create only 4.5 mm of the quilter's cotton which is a single part of the fabric that was tested in Konda et al's research study [21].

3.2.1 Simulation setup

To design the model to be accurate of 80 TPI woven fabric, 1 mm of cotton 152 TPI has 3 yarns [39], resulting in 4.5 mm of 80 TPI has 7 yarns. To generate the model geometry, place two adjacent weft lines on the centerline. And make the weft and warp fibers the same diameter. Utilize equations (1) to (8) with the specified values and construct the geometry in Spaceclaim. Aware not to overlap the generated fibers during the construction process. As a result, some adjustments may be necessary to avoid skewness. The fibers' warp and weft diameters are both 0.27 mm. The distance between the warp cover and the weft is 0.642 mm and the contact angle is 29.205 degrees. The model was shown in Figure 3.2 and the parameters used to generate the fiber geometry are shown in Table 3.2.

Table 3.2 The parameters used to generate fiber geometry 80 TPI.

Parameters	Value
D_j, D_w	0.27 mm
h_j, h_w	0.27 mm
c_j, c_w	0.0992 mm
l_j, l_w	0.7066 mm
θ_j, θ_w	29.205 degree
L_j, L_w	4.9465 mm
N_j, N_w	7 n
A, B	4.5 mm

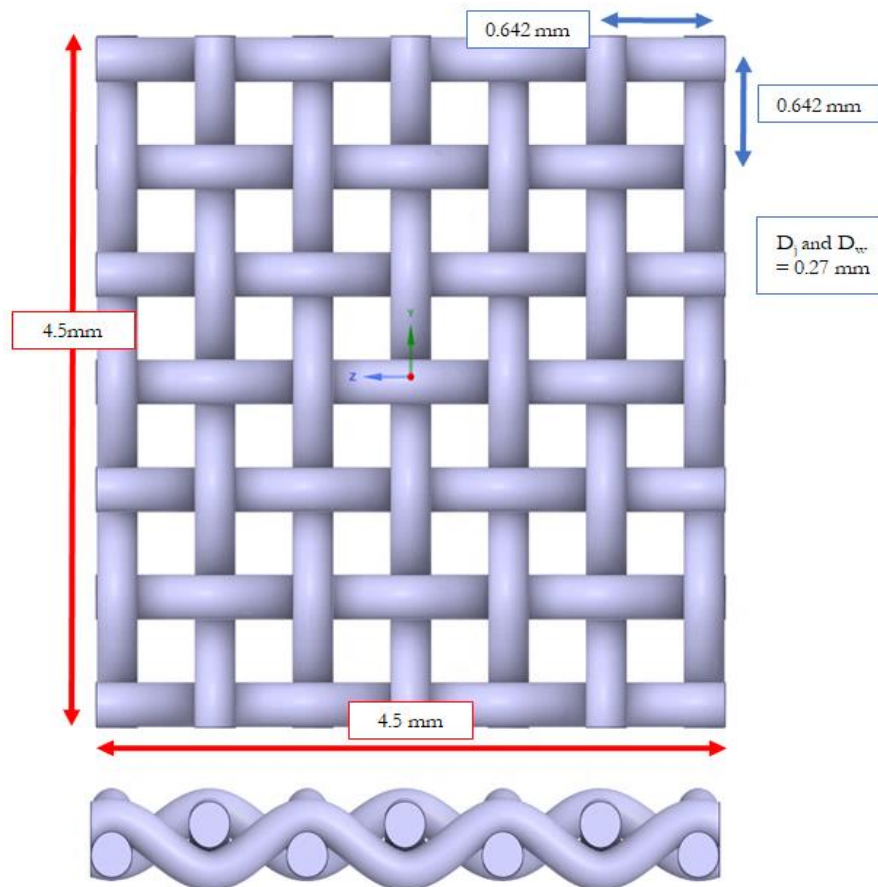


Figure 3.2 The plain weave model in this simulation has a warp and weft diameter of 0.27 mm, a distance between the warp cover and the weft of 0.642 mm, and a contact angle of 29.205 degrees.

จุฬาลงกรณ์มหาวิทยาลัย
CHULALONGKORN UNIVERSITY

3.3 Computational fluid domain

The purpose of this study is to examine the filter performance of fibers in a fluid area with dimensions of 4.5 mm x 4.5 mm x 6.12 mm. To achieve this, a fiber model and simulated air filtration. However, for the purpose of analysis, the fiber model was later removed from the fluid domain. It is assumed that the flow field has no impact on the inlet and outlet calculation zones, which were predetermined. In their previous study, Hosseini and Tafreshi [40] investigated air filtration simulations with varying inlet and outlet media lengths. They found that an inlet media length of 20 times the fiber diameter and an outlet media length of 5 times the fiber diameter produced optimal results. In this current work, however, the inlet and outlet are placed at a distance of 10 times the

diameter of the fiber to prevent any object or surface from obstructing or disrupting the smooth and continuous movement of fluid. The thickness of the fiber used in this study is 0.72 mm. The domain dimension is shown in Figure 3.3.

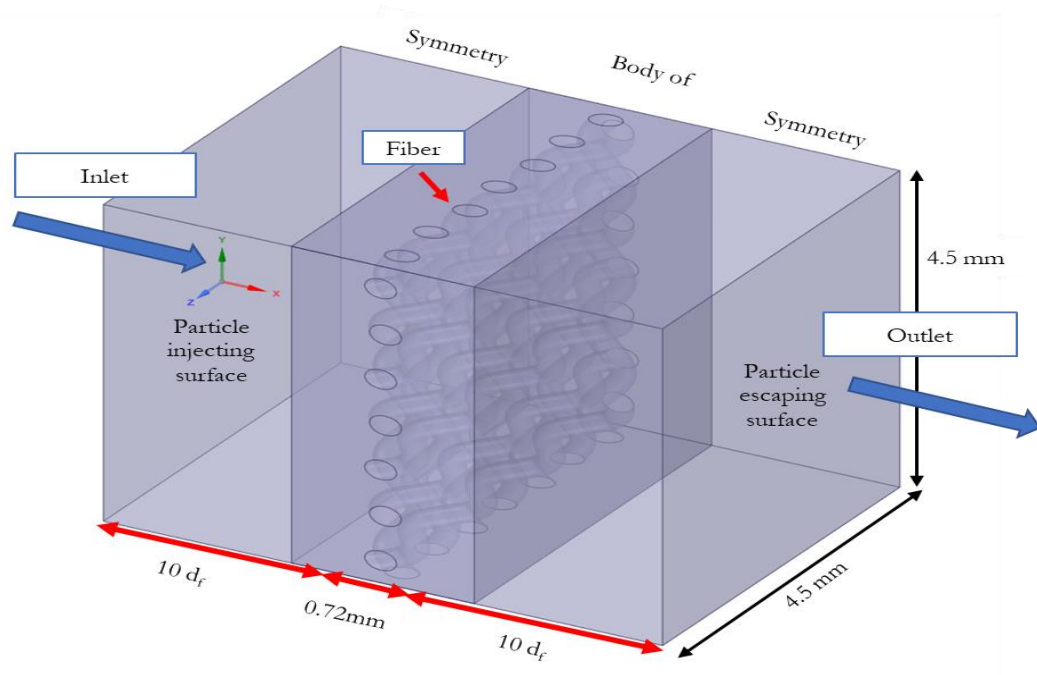


Figure 3.3 Simulation domain and boundary conditions (SVF = 27.16%, $d_f = 270 \mu\text{m}$).

Table 3.3 Parameter setting of grids.

Case	Element size (mm)	Body of influence size (mm)	Fiber face size (mm)	Element number
1	0.3	0.2	0.2	316500
2	0.3	0.1	0.1	603649
3	0.2	0.1	0.1	608185
4	0.15	0.1	0.1	631343
5	0.1	0.06	0.06	1888715
6	0.08	0.06	0.06	2036121
7	0.08	0.05	0.05	3133536
8	0.08	0.05	0.04	3367060
9	0.08	0.04	0.04	5453960
10	0.06	0.04	0.04	5825664

3.4 Mesh

To simulate the fiber zone, a mesh consisting of 3.4 million tetrahedral elements was generated. The element size was set to 0.08 mm for the mesh, which was considered suitable for the modeling purpose. However, due to the presence of curves and overlapping parts in the fiber zone, a body of influence was created to reduce the element size by approximately 0.05 mm, resulting in a finer mesh with better quality. In addition, to ensure the accuracy of the simulation, the face surface of the fiber element was set to 0.04 mm. The average value of skewness was obtained to evaluate the mesh quality. The test showed a value of 0.21, which is within an acceptable range. This indicates that the model's mesh quality is appropriate for the intended purpose, and the simulation results may be relied on with fair confidence. Overall, the usage of an optimized mesh with proper element size and body of effect has aided in ensuring the simulation's correctness and dependability. The tetrahedral mesh is shown in Figure 3.4.

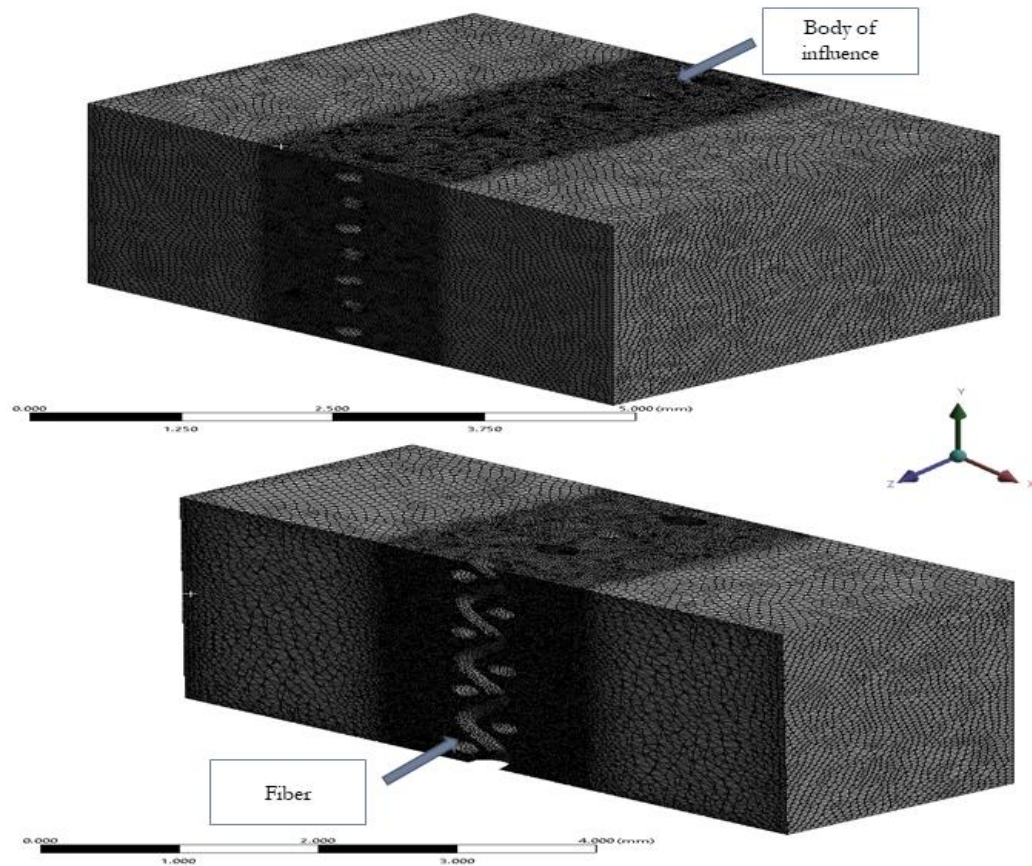


Figure 3.4 Tetrahedral mesh of the model with max size of element is 0.08 mm and Body of influence size 0.04 mm.

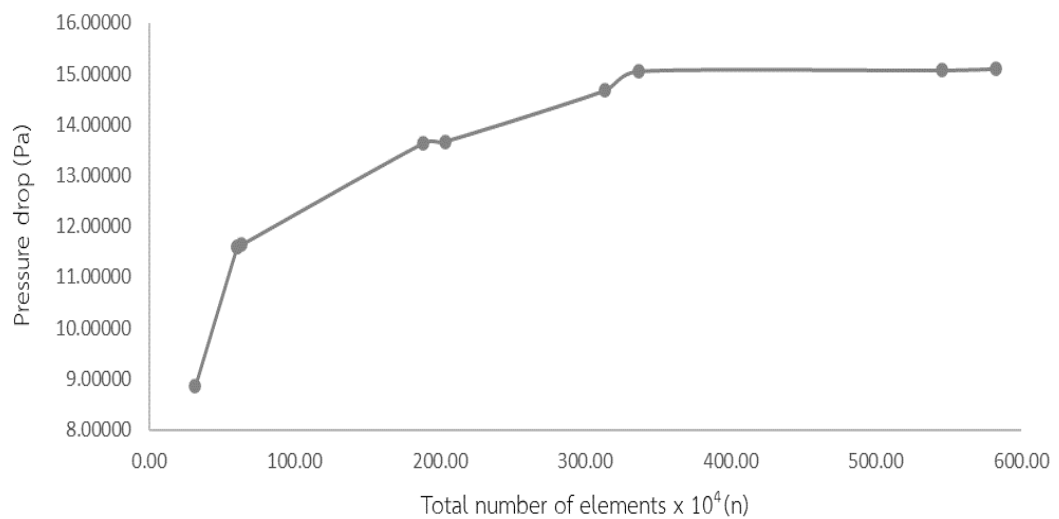


Figure 3.5 The effect of computational domain size on pressure drops.: Total number of elements compare to the pressure drop.

3.4.1 Mesh independent test

It is critical to investigate if the size of the mesh employed in the simulation influences the reliability and accuracy of numerical findings. The mesh density in Fluent simulations is important in influencing the accuracy of the numerical calculations. The greater the mesh density, the more exact the numerical outputs. The study investigates the link between the pressure drop and the total number of components in the model to attain this degree of precision. As indicated in Table 3.3 and Figure 3.5, the simulation observed pressure decreases during the filtering process to achieve this. The results showed that as the mesh density grew, the pressure drop tended to remain steady, indicating that the mesh size had no major effect on the numerical results. As a result, the researchers chose a mesh with 3,367,060 components for the simulation since it gave a sufficient degree of accuracy without straining computer resources excessively. It is worth mentioning that picking an acceptable mesh size for simulation might be difficult. This is because a coarse mesh might produce erroneous numerical results, but a fine mesh can be computationally expensive and time-consuming to process. As a result, great thought must be paid to selecting a mesh size that is appropriate for the simulation's intended purpose. Overall, the study's findings emphasize the relevance of mesh density in Fluent simulations and the necessity for careful thought when selecting an acceptable mesh size.

3.5 Gas phase model

The governing equations of gas phase model are typically the Navier-Stokes equations, which describe the conservation of mass, momentum, and energy in a fluid. These equations are a set of partial differential equations that describe the time evolution of fluid flow and can be used to model a wide range of physical phenomena, from simple laminar flows to complex turbulent flows. For the calculation of Reynolds number to determine the flow type can be written as follows:

$$Re = \frac{\rho d \bar{u}}{\mu} \quad (9)$$

Where \bar{u} is the flow velocity, d is the diameter of fiber, ρ is the density of fluid and μ is the dynamic viscosity. The Reynolds number of fluid velocity 0.05 m/s to 0.75 m/s at is between 0.9 to 15. Thus, the flow of the air in this simulation is laminar flow.

3.5.1 Mass conservation equation

In the simulation, the Reynolds number was small (less than 15). The flow of fluid was Laminar flow. The mass conservation equation or continuity equation can be written as follows.

$$\nabla \vec{u} = 0 \quad (10)$$

Where \vec{u} is the flow velocity and ∇ is the gradient operator.

3.5.2 Momentum conservation equation

The momentum conservation equation (Navier-Stokes) or Newton's second law equation can be written as follows:

$$\nabla \cdot (\rho \vec{u} \vec{u}) + \nabla p = \mu \nabla^2 \vec{u} + \rho \vec{g} \quad (11)$$

where p is the static pressure, μ is the molecular viscosity, $\rho \vec{g}$ is the gravitational body force.

3.6 Discrete phase model

Fluent's discrete phase model employs the Euler and Lagrangian methods to simulate gas-solid two-phase flow [41, 42]. The trajectory of the particle is determined by Newton's second law of motion, which includes drag, gravity force, Brownian force, and Saffman's lift force, which is calculated by integrating the particle's force balance equation:

$$\frac{\partial \vec{u}_p}{\partial t} = F_D (\vec{u} - \vec{u}_p) + \frac{\vec{g}(\rho_p - \rho)}{\rho_p} + \vec{F}_l \quad (12)$$

Where \vec{u}_p is the particle velocity, ρ is the fluid density, ρ_p is the particle density which will be considered as the density of sodium chloride that equals 2170 kg/m³, \vec{F}_l is the additional acceleration terms. The expression of F_D or drag force is as follows:

$$F_D = \frac{18\mu}{\rho_p d_p^2 C_C} \quad (13)$$

$$C_C = 1 + Kn_p (1.257 + 0.4e^{-1.1/Kn_p}) \quad (14)$$

Where d_p is the particle diameter, C_C is the Cunningham correction factor [43], $Kn_p = \lambda/d_p$ is the Knudsen number, λ is the mean free path of the gas molecule. Since the Reynolds number of submicron particles is low, Saffman's lift force (F_S) [44] should be calculated. The expression of F_S is as follows.

$$F_S = \frac{2K\nu^{1/2}\rho d_{ij}}{\rho_p d_p (d_{ik}d_{kl})^{1/4}} (\vec{u} - \vec{u}_p) \quad (15)$$

Where $K = 2.594$, ν is kinematic viscosity of fluid and d_{ij} is the deformation tensor. And when the particle diameter is small Brownian force also should be considered too. But when the velocity is increased the effect of Brownian force can be decreased. The expression of F_B is as follows.

$$F_B = \xi \sqrt{\frac{216\mu k_B T}{\pi \rho_p^2 d_p^5 C_C \Delta t}} \quad (16)$$

Where k_B is the Boltzmann constant, ξ represents a random number in a standard normal distribution with a zero mean and a variance of 1, T is the thermodynamic temperature, Δt is the time step.

For micron particles, the Spherical law of drag force is used, and the impact of gravity is considered [29]. The expression of the drag force is as follows:

$$F_D = \frac{3\eta C_D Re}{4\rho_p d_p^2} \quad (17)$$

$$\overline{Re} = \frac{\rho d_p |\vec{u}_p - \vec{u}|}{\mu} \quad (18)$$

$$C_D = \frac{24}{Re} (Re \leq 0.1) \quad (19)$$

$$C_D = 3.69 + 22.73\sqrt{\overline{Re}} + 0.0903\sqrt{\overline{Re}^2} (0.1 \leq Re \leq 1) \quad (20)$$

Where \overline{Re} is the relative Reynolds number, C_D is the drag coefficient. For relative Reynolds number less than 0.1 the drag coefficient $C_D = 24/Re$ is used and the same as Stokes Cunningham drag law. Moreover, when the relative Reynolds number is between 0.1 and 1, the spherical drag law provides a more precise description of the drag coefficient C_D .

This simulation was run in steady-state mode, with the computation domain considered to be laminar flow due to the low Reynolds number. The rate of breathing rises as the intensity of the exercise increases. where the minimum and maximum effort rates are 6 and 85 lpm, respectively [35]. The flow velocity was determined for the 190 cm² mask area [36] and ranged from 0.5 cm/s to 7.5 cm/s, respectively.

3.7 Analytical model

3.7.1 Pressure drop

Pressure drop of the fibrous media is an important factor. The flow of air through the fibrous media is a laminar, the expression of pressure drop follows Darcy's law. The Darcy-Forchheimer equation, which has been extensively used in the literature to explain the pressure drop of fibrous media is as follows [31]:

$$\frac{\Delta p}{L} = f(\alpha_f) \frac{\mu}{a_f^2} \quad (21)$$

Where Δp is the pressure drop, α is the solid volume fraction of fibrous media, L is the filter medium thickness and $f(\alpha)$ is the dimensionless drag coefficient as a function of SVF. Many formulas for $f(\alpha)$ based on different theories exist, for example, Happel [32], Kuwabara [33], and others. The expression of Happel is simply defined as follows:

$$f(\alpha) = \frac{16\alpha}{-0.5 \ln \alpha - 0.5 \frac{1-\alpha^2}{1+\alpha^2}} \quad (20)$$

Kuwabara was given on the basis that the surface curl of cylinder was 0, more precisely if the horizontal and vertical distances between fibers are equal. The expression of Kuwabara is as follows:

$$f(\alpha) = \frac{16\alpha}{-0.5 \ln \alpha + \alpha - 0.75 - 0.25\alpha^2} \quad (21)$$

The two popular expressions, by Davies [34] and Rao [35]. Both are conducted experiments and numerical simulations to investigate the pressure drop of fibrous medium, respectively. The expression as follows:

$$f(\alpha) = 64\alpha^{1.5}(1 + 56\alpha^3) \quad (22)$$

$$f(\alpha) = 2.653\alpha + 39.34\alpha^2 + 144.5\alpha^3 \quad (23)$$

3.7.2 Filtration efficiency

The efficiency of filtration may be estimated by using the following equation to find the number of particles that vanish from the air after filtering:

$$E = 1 - \frac{N_{out}}{N_{in}} \quad (24)$$

Where N_{in} is the total amount of particle inlets and N_{out} denotes the total amount of particle outlets.

It is the usage of particles before and after the experiment to determine which type of filter cloth provides the best results. The theory of single-fiber efficiency (SFE) evaluates the filtration efficiency of fiber filters as a homogeneous model with a centered fiber [45]. The equation is as follows.

$$E = 1 - \exp\left(\frac{-4\alpha\eta}{\pi d_f(1-\alpha)}\right) \quad (25)$$

E is the filtration efficiency and η is the total filtration efficiency of a single fiber. which can be written in terms of inertial impaction and diffusion are as follows.

$$\eta = 1 - (1 - E_I)(1 - E_R)(1 - E_D) \quad (26)$$

Where E_I is the efficiency due to inertial impaction, E_R is the efficiency due to interception and E_D is the efficiency due to diffusion. And shown as follows: [46] [47]

$$E_I = \frac{Stk^3}{Stk^3 + 0.77Stk^2 + 0.22} \quad (27)$$

$$E_R = 0.6 \frac{1-\alpha}{Ku} \frac{R^2}{(1+R)} \quad (28)$$

$$E_D = 2.6 \left(\frac{1-\alpha}{Ku}\right)^{1/3} Pe^{-2/3} \quad (29)$$

$$Stk = \frac{\rho_p d_p^2 C_c V}{18\mu d_f} \quad (30)$$

$$R = \frac{d_p}{d_f} \quad (31)$$

$$Pe = \frac{V d_f}{D} = \frac{3\pi\mu V d_p d_f}{k_B C_c T} \quad (32)$$

$$Ku = \frac{-(\ln\alpha)}{2} - \frac{3}{4} + \alpha - \frac{\alpha^2}{4} \quad (33)$$

Where R is the intercept coefficient, Ku the Kuwabara hydrodynamic factor, Stk the Stokes number, Pe the Peclet number, D the diffusion coefficient, T the absolute temperature of fluid, C_c the Cunningham correction factor and d_p the particle diameter.

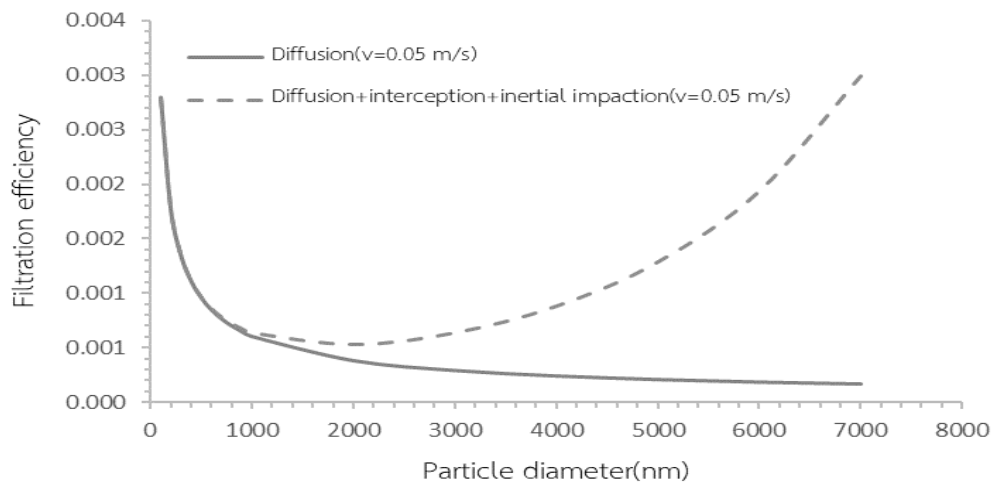


Figure 3.6 A comparison based on analytical model between the three capture mechanisms of Brownian diffusion, interception, and inertial impaction (Plain weave, $d_f = 270 \mu\text{m}$, SVF = 27.16%).

Figure 3.6 and 3.7 both show the filtration efficiency of analytic calculations theoretical for 80 TPI (fiber diameter 270 micron) and 300 TPI (fiber diameter 65 micron) respectively. The observed pattern in the two plots indicates that Brownian diffusion is more important in smaller particle sizes, but its importance decreases as particle sizes increase. Particle size and other factors influence particle diffusion efficiency. Larger particles have a decreased diffusion efficiency for a variety of reasons, including:

Increased mass: Larger particles have a higher mass than smaller particles. Because of their higher mass, they are more prone to gravity settling, which means they will settle or sediment more quickly in a fluid media. As a result, the pace of diffusion slows.

Longer diffusion path: Diffusion happens when particles move randomly and clash with other particles, causing them to spread out. Larger particles have a longer diffusion path due to their larger size. This longer path increases the probability of collisions and lowers diffusion efficiency overall.

Increased drag forces: Larger particles experience greater drag forces as they move through a fluid medium. These drag forces resist the motion of particles and can slow

down their diffusion. The drag forces are influenced by factors such as particle size, shape, and fluid viscosity.

Increased drag forces: Brownian motion is the random motion of particles caused by collisions with fluid molecules. It is an essential mechanism for diffusion. However, larger particles experience less Brownian motion compared to smaller particles because their increased mass makes it harder for them to be influenced by the rapid, random movements of fluid molecules.

Overall, larger particles have lower diffusion efficiency due to their increased mass, longer diffusion path, higher drag forces, and limited Brownian motion. These factors hinder their ability to disperse and spread out effectively in a fluid medium.

When the effects of interception and inertial impaction, which are dominating mechanisms in larger particles, are considered, there is an increase trend in filtering efficiency with larger particle sizes.

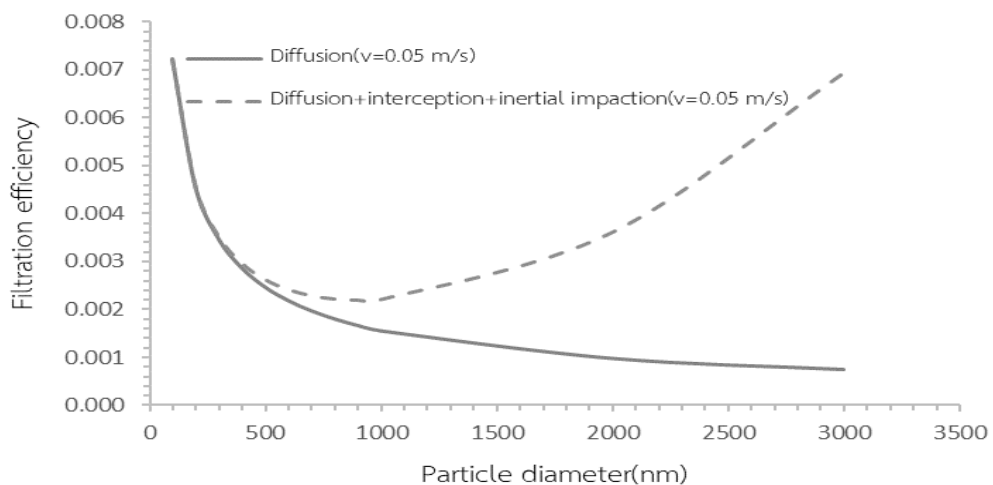


Figure 3.7 A comparison based on analytical model between the three capture mechanisms of Brownian diffusion, interception, and inertial impaction (Plain weave, $d_f = 65 \mu\text{m}$, SVF = 27.16%).

3.8 Boundary condition

The ANSYS FLUENT with Laminar flow model was utilized for conducting a steady-state flow simulation. The boundary conditions at the entrance of the system determine the airflow velocity associated with four distinct exercise intensity levels. By precisely specifying the velocity at the inlet, we can effectively track and compute the path of particles as they traverse the fiber medium. Additionally, the exit of the domain is intentionally designed to remain open, enabling the natural dispersion of particles and facilitating their outflow from the system. The boundary conditions for the inlet and outlet were set to "velocity inlet" and "pressure outlet," respectively, to account for the incompressible flow. Additionally, the boundary conditions for the inlet and outlet were set to "escape," which means that the particle disappears after it encounters the boundary, while the fibers' boundary conditions were set to "trap." In other words, the trajectory calculations are terminated after the collision, and the fate of the particle is counted as trapped. These boundary conditions were applied to evaluate the filtration efficiency of the fiber model.

To prevent disturbing the fluid flow, the inlet and outlet boundary conditions were placed 10 times the diameter of the fibers away from them. This setup allowed for an undisturbed flow field, and the fluid could be considered completely developed within the control domain. To simulate respiratory droplets and aerosols, sodium chloride aerosol particles were used in this simulation, as was done in Konda's work [21]. The NaCl aerosols were modeled using the Discrete Phase Model (DPM), with surface injection and particle concentrations estimated based on Konda's upstream NaCl aerosol concentration and injected as a mass flow rate. All particles were considered inert, and the total mass flow rate of NaCl aerosols was calculated using particulate matter concentrations ranging from 6 nm to 220 nm in the air [48].

To achieve the filtering mechanism, two functions were activated in the Discrete Phase Model: Saffman's lift force and Brownian motion. The buoyancy force was also enabled in conjunction with gravity. The outlet was defined as a pressure outlet boundary condition with a pressure equivalent to the atmospheric pressure. Furthermore, the computational domain's walls were constrained by symmetry boundary conditions, which did not have a significant impact on the simulation results since the fiber media of the

entire fibrous filter was used, and there was no significant lateral airflow present in the simulation region. These details were reported in a previous study [49]. The Knudsen number's low value indicates that the flow is a stoke flow.

Fluent's Discrete Phase Model (DPM) is capable of simulating particles in a continuous flow regime. The DPM is a Lagrangian technique that monitors individual particle movement in a fluid flow. The technique considers particles as distinct entities that are carried through the fluid by following the fluid velocity field. The continuum flow regime indicates that the particle volume fraction is significantly smaller than the fluid volume, and the presence of particles has a minimal impact on the flow field [50]. As a result, in this regime, the fluid flow is considered continuous. Therefore, the slip effect can be ignored, and the fibers surface is assumed as a no-slip boundary condition. This is due to fabric masks' ability to filter out quite large particles. For this study, a total of approximately 10000 particles were employed to track. To determine the filtration efficiency of each particle on the weave pattern of the woven cloth.

3.8.1 Limitation of this work

Since this research involves setting the entrance and exit of the domain to be open to the air, it is important to note that in reality, the mask is a closed part. Therefore, the exit of the domain should be an impermeable area to prevent air from passing through. This will allow for the study of the airflow after it impacts the mask and disperses to the sides, rather than potentially affecting the filtration, which may change due to altered airflow after impact. Additionally, this research does not consider the leakage of air that may occur around the cheeks or chin during actual breathing while wearing the mask. This aspect may need to be considered in future experiments. Finally, air moisture, which can cause water adsorption, may need to be integrated into the mixture species model to introduce adsorption filtering processes that could potentially modify filtration performance.

3.9 Investigation of weave-patterns effect on filtration performance

In this study, the filtration performance of filter cloths with three basic weave patterns, namely plain, twill, and satin weave, was investigated. The air flow passing through the fiber changes as the fiber moves from its initial position, resulting in particle movement shifts and potentially different particle filtering outputs for each weave pattern. However, the effect of particle deposition on fiber size was not considered in this experiment. To analyze the effect of different patterns, the fluid domain area was limited to 4.5 mm, which contains around 7 fibers on each side. The satin and twill weaves were modeled with the same fiber diameter and contact angle as the plain weave, but their unique patterns resulted in different weaves. The fiber of twill weave and satin weave are shown in Figure 3.9. Thus, both twill and satin weave fibers are simulated as plain weave fibers under the same conditions to determine which has superior filtration performance. The simulations were run at airflow velocities of 0.05, 0.18, 0.27, and 0.75 m/s, representing the increasing intensity of exercise. To improve the design of cotton masks that may be worn while exercising.

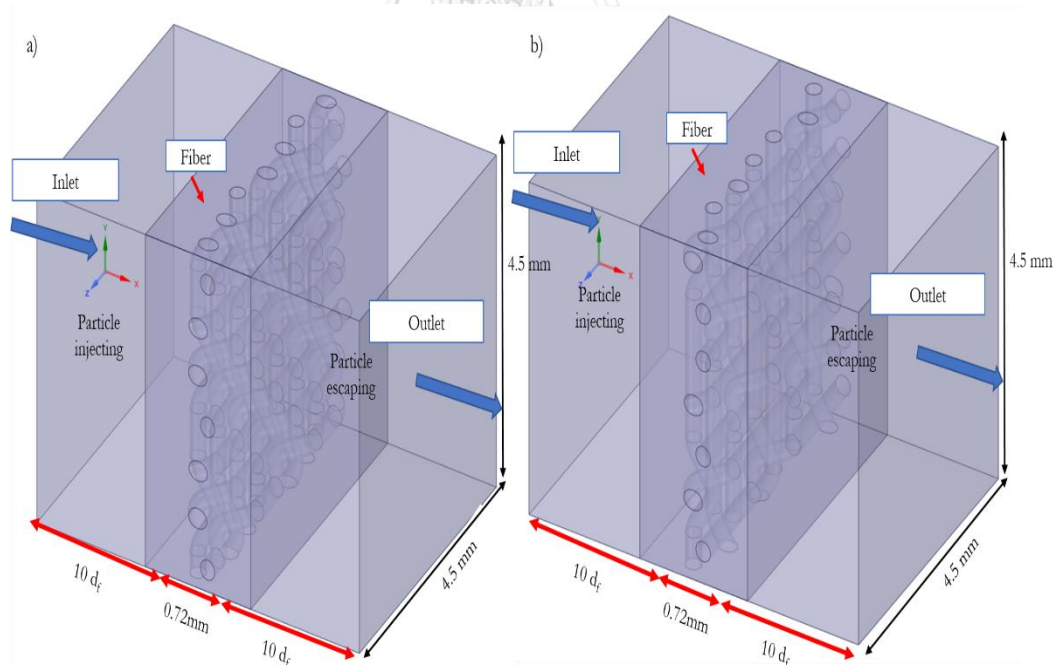


Figure 3.8 Simulation domains: a) twill weave, b) satin weave Both weaves have the same parameters as plain weave.

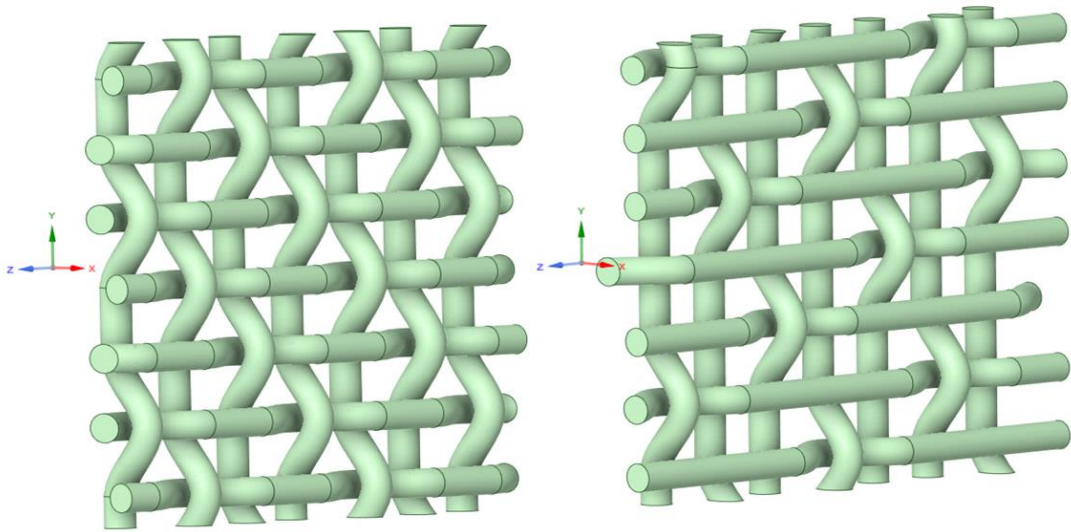
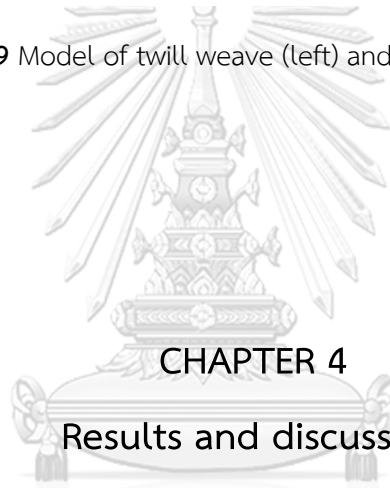


Figure 3.9 Model of twill weave (left) and satin weave (right)



CHAPTER 4

Results and discussion

จุฬาลงกรณ์มหาวิทยาลัย

CHULALONGKORN UNIVERSITY

4.1 Model validation

Model validation is an important step in ensuring the reliability and correctness of the computational model in the investigation of the weave-pattern effect on filtration performance of woven filter cloths using computational fluid dynamic modeling. The validation step entails testing the model's performance on a new set of data, which includes pressure drop and filtration efficiency measurements for filter cloths with various weave patterns. During the validation phase, the accuracy and generalization capabilities of the model can be tested by comparing projected and measured pressure drop and filtering efficiency data. The model's settings can then be fine-tuned to improve filtration efficiency and reduce pressure drop by optimizing filter cloth design. Validating the model with pressure drop and filtration efficiency data is critical for developing a trustworthy

computational model that can provide significant insights into the design and optimization of filter cloths for diverse applications.

4.1.1 Pressure drop

To compare the simulation results of pressure drop at different filtration velocities for a plain weave model with a diameter of 0.065 mm and 300 TPI to the Happel and Davies models, the results of simulation of the model created in this study have the pressure drop close to the Happel and Davies models. The model has 300 TPI and a diameter of 0.065 mm. The model was created using Equations (1) through (8). The pressure drops and filtration efficiency numbers produced from the simulation were identical to those obtained from the Happel Davies model, which was established from experiments measuring pressure drops in packed or fixed beds. The studies comprised measuring various fluid velocities and void percentages, and the experimental data was used to create an empirical equation linking pressure drop to Reynolds number and void fraction.

The Davies model considers the additional factors of Brownian motion and gravitational settling, apart from the viscous drag force. The equation is valid for Reynolds numbers ranging from 0.1 to 100 and void fractions ranging from 0.4 to 0.95. The Happel equation is not derived directly from experiments, but it is based on theoretical analysis of the motion of a spherical particle in a fluid.

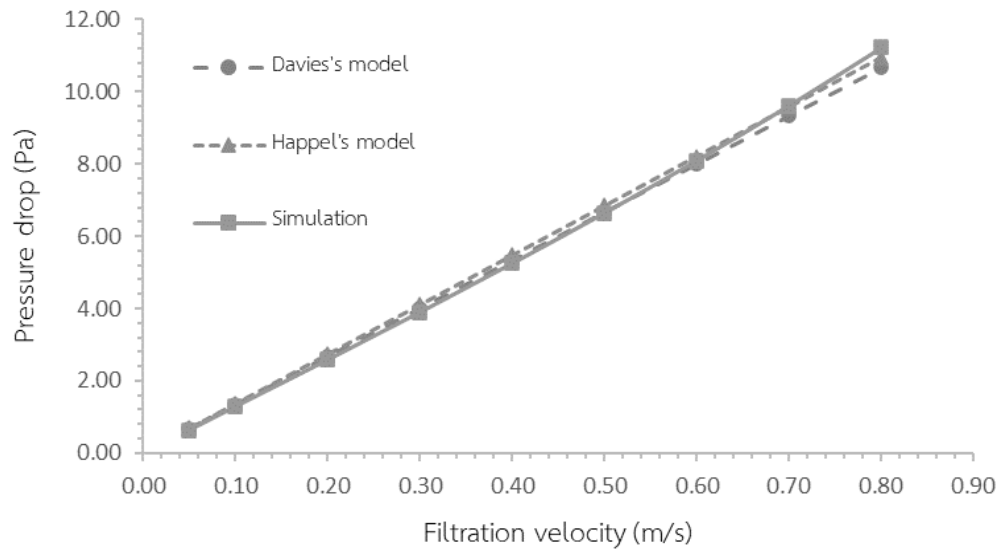


Figure 4.1 pressure drop comparing the experiment and simulation (plain weave model with 0.065 mm diameter and 300 TPI).

In Figure 4.1 presents some very compelling results. The pressure drop versus filtration velocity of this simulation model was compared to that of an experimental model (the Davies model) and a theoretical model (the Happel model) and found that the outcomes were remarkably similar. These findings demonstrate that our simulated fiber model can accurately predict the filtering performance of real filter cloths. Overall, these results provide strong validation for the use of our simulation model to explore the impact of different weave patterns on the filtration efficiency of woven filter cloths.

4.1.2 Filtration efficiency

The simulation's accuracy was confirmed by comparing its results to the data obtained from Konda's research, which used fabric of the same weave, thread count per inch (TPI), and a flow rate of 1.2 CFM. The study compared the efficiency of Quilter's 80 TPI cotton mask in filtering particles of different sizes with simulation results. In this investigation, the model was produced in the same way as Konda's work and under the same conditions. NaCl aerosols were employed to create particles of varying sizes, as follows: 28, 37, 49, 65.5, 87.5, 116.5, 155.5 and 450 nm. As shown in Figure. 4.2.

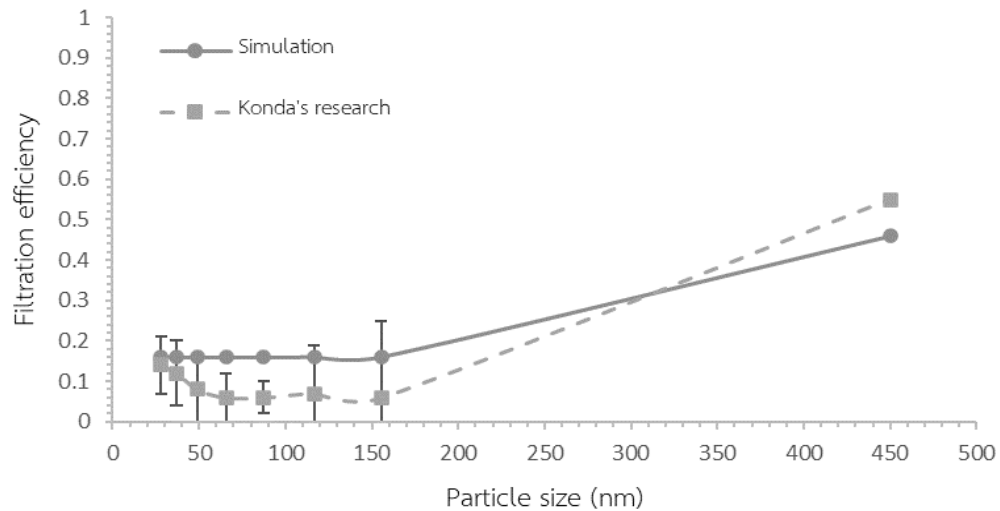


Figure 4.2 The simulation results of filtration efficiency at flow rate 1.2 CFM with the same plain weave, TPI, fiber diameter, and aerosol type as Konda's research are compared.

The filtering effect of the plain weave model was related to particle diameter. The particle injection was injected to the DPM as surface type with a flow rate of 1.2 CFM. The modeling findings for filtering efficiencies are compared to the experiment results. The results reveal that simulation filtration efficiencies outperform experiment filtration efficiencies. The interplay of several capture methods explains it [51, 52]. Because the modeling technique does not include particle reflection off the fiber surface, the numerical findings are significantly higher than the experimental values. However, with particle diameters of 450, they are less than the data. Disagreements between DPM model findings and experimental data for particles of varying sizes might be caused by a variety of variables. One probable explanation is that the assumptions and simplifications in the DPM model do not adequately account for the complicated fluid-particle interactions that occur in actual systems. Differences in operating circumstances between the simulation and experiment may also have an impact on the accuracy of the results. Despite these constraints, the 450 nm particle filtering efficiency follows a similar pattern to the experimental data.

4.2 Flow field distribution

In the filtration process of fibrous filters, the primary source of resistance is the fluid flow through the pores. Figure 4.3 shows the internal flow field of fibrous media of plain weave with an SVF of 27.16% and a fiber diameter of 270 μm at filtration velocities of 0.05, 0.18, 0.27, and 0.75 m/s. As the filtration velocity increases, the flow field distribution in the fibrous media also changes, which can be attributed to the increase in Stokes number. This observation highlights the importance of considering filtration velocity when designing and optimizing fibrous filter media for various applications. Figures 4.4 and 4.5 demonstrate the internal flow field of satin weave and twill weave fibrous media, respectively.



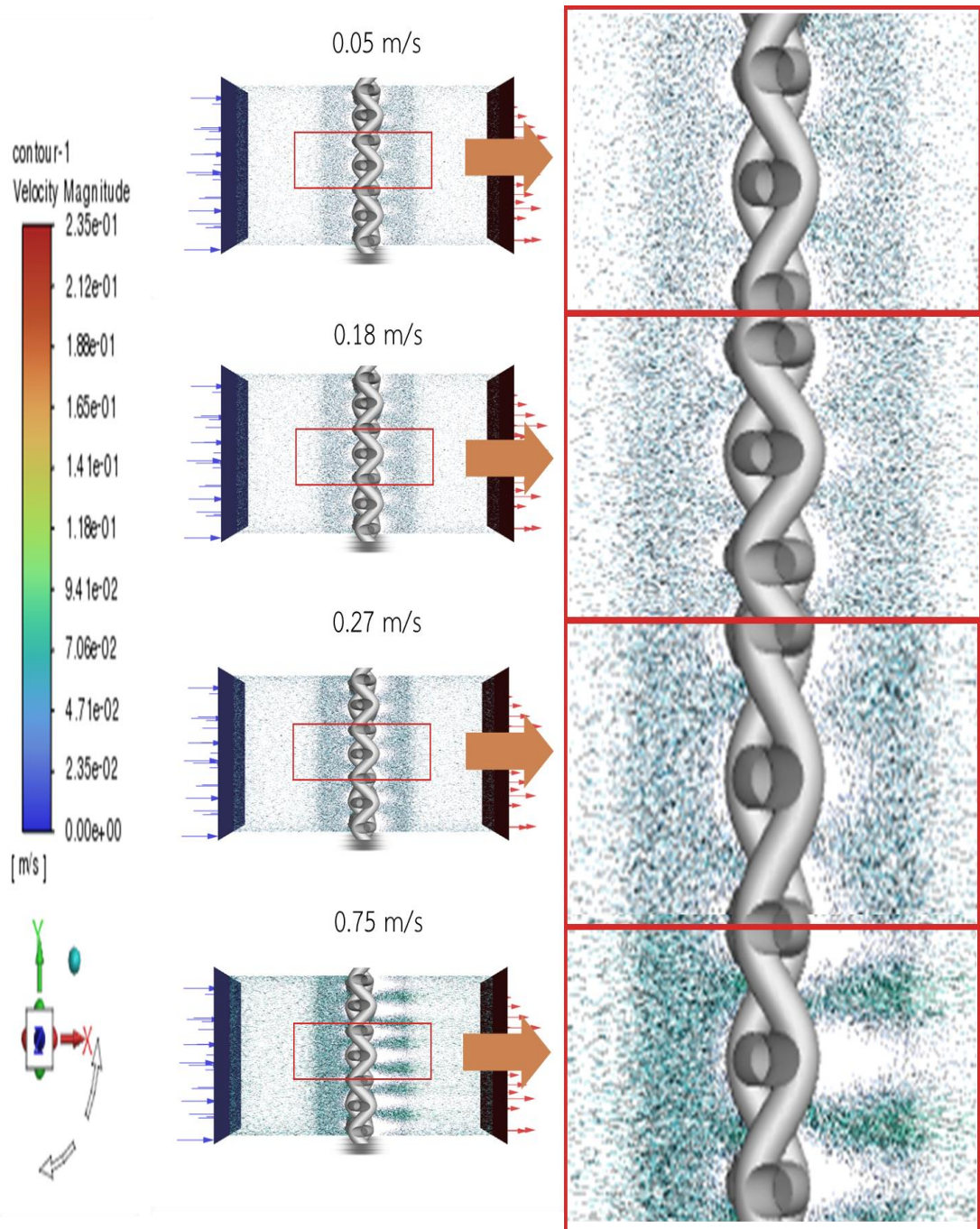


Figure 4.3 Flow field of fibrous media with different filtration velocity (Plain weave 300 TPI SVF = 27.16%, $d_f = 65 \mu\text{m}$).

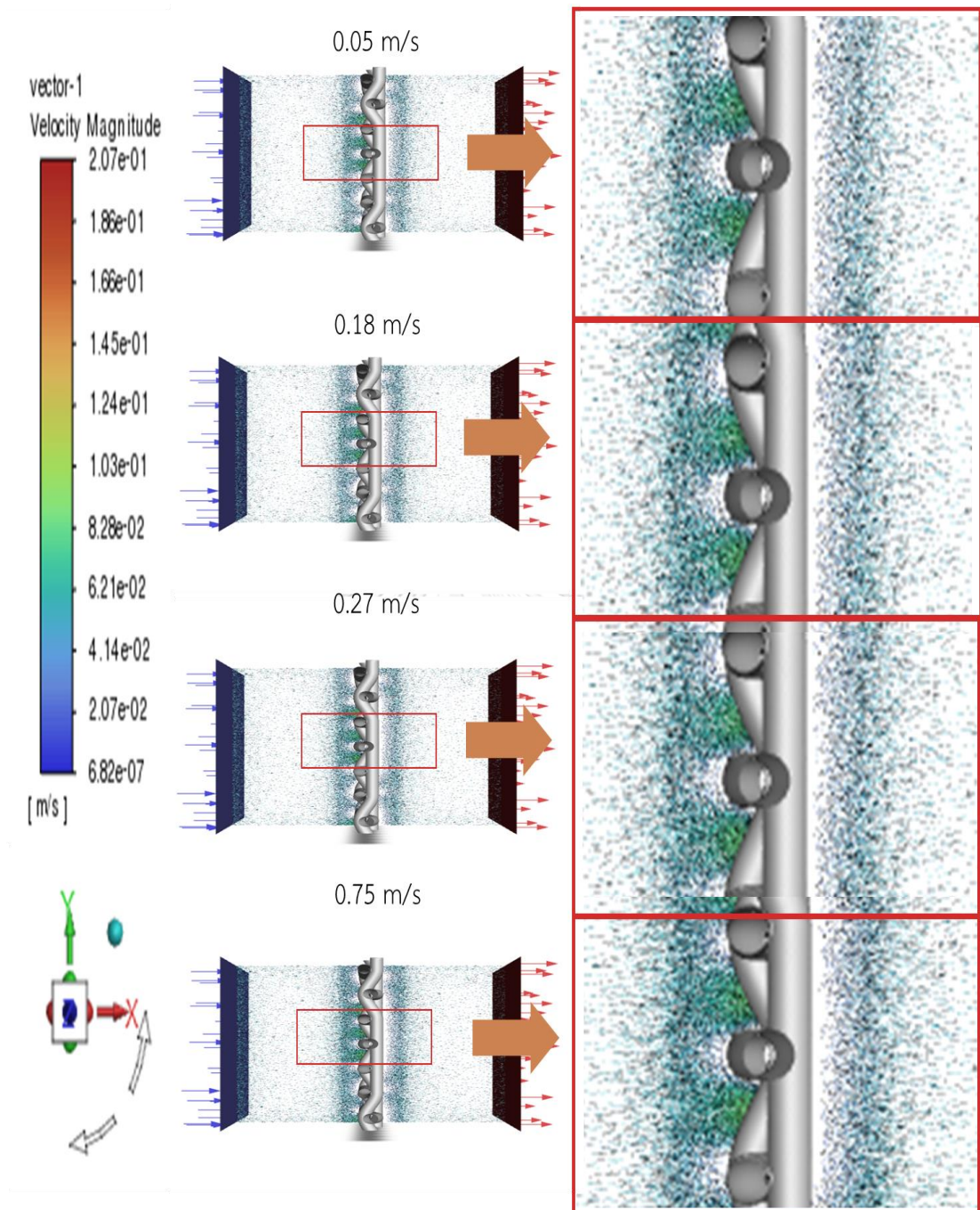


Figure 4.4 Flow field of fibrous media with different filtration velocity (Satin weave 300 TPI
SVF = 27.16%, $d_f = 65 \mu\text{m}$).

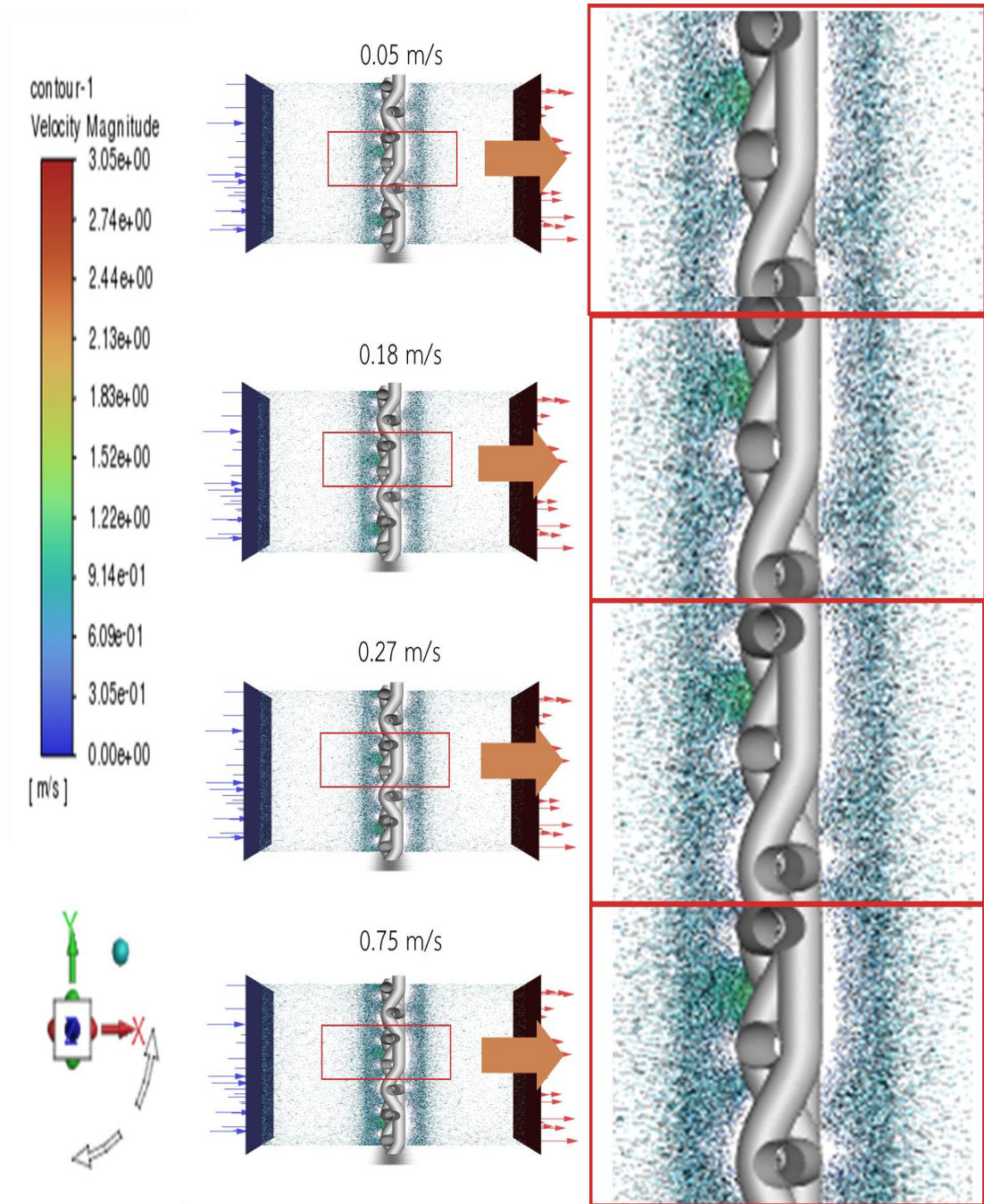


Figure 4.5 Flow field of fibrous media with different filtration velocity (Twill weave 300 TPI
SVF = 27.16%, $d_f = 65 \mu\text{m}$).

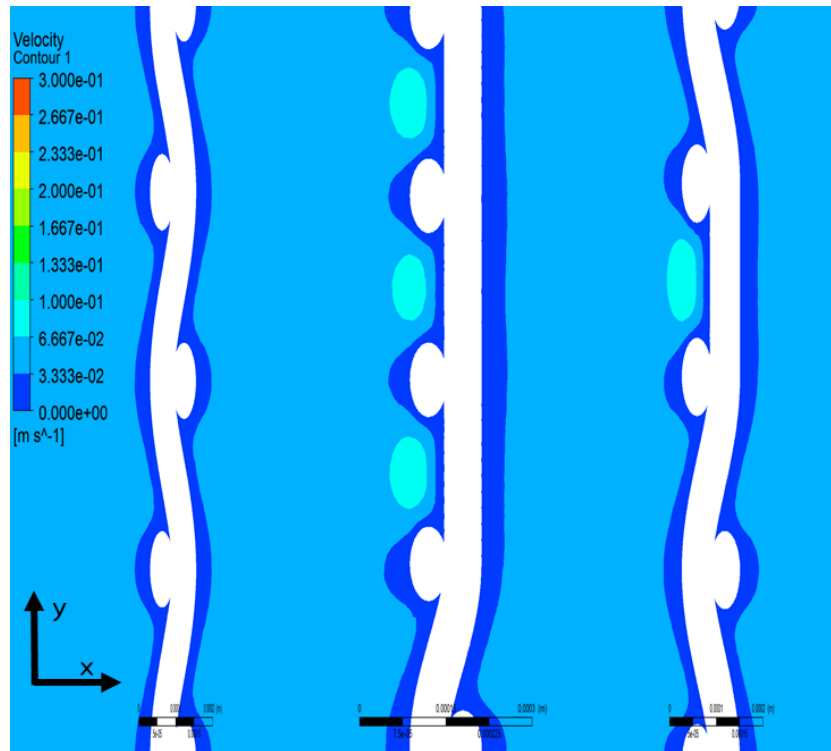


Figure 4.6 Velocity contour at 0.05 m/s for plain weave on the left, satin weave on the center, and twill weave on the right.

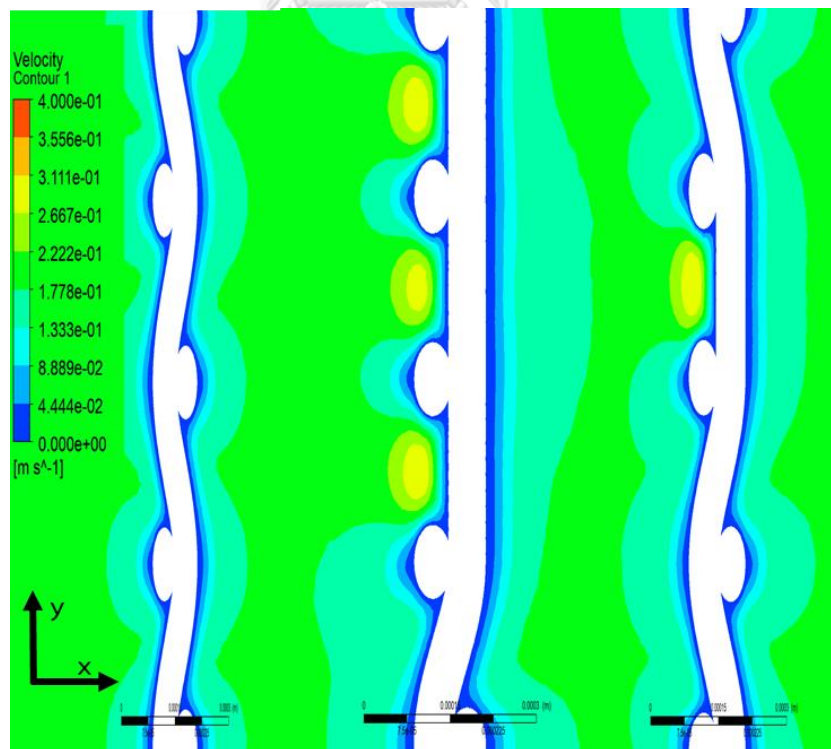


Figure 4.7 Velocity contour at 0.18 m/s for plain weave on the left, satin weave on the center, and twill weave on the right.

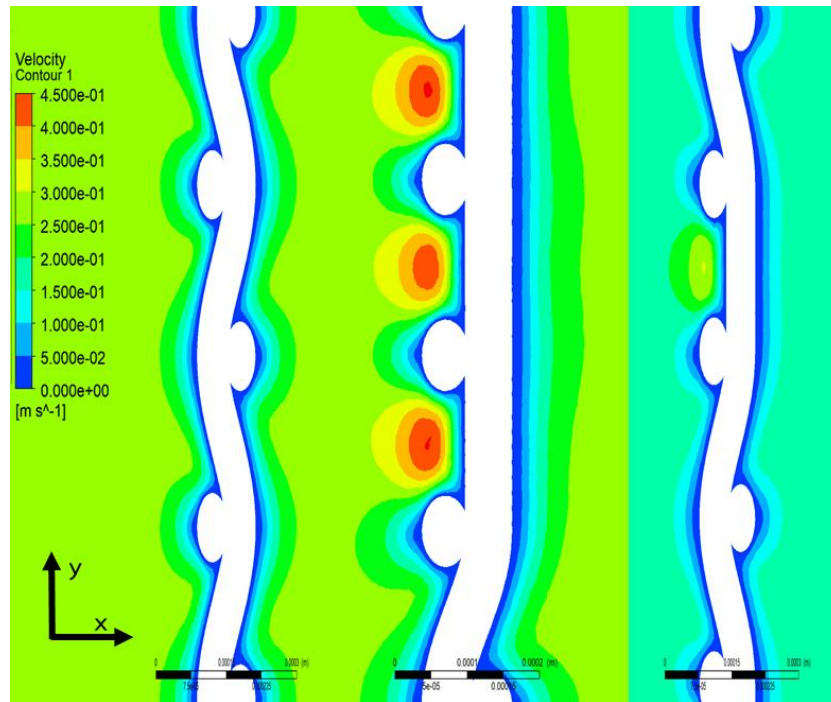


Figure 4.8 Velocity contour at 0.27 m/s for plain weave on the left, satin weave on the center, and twill weave on the right.

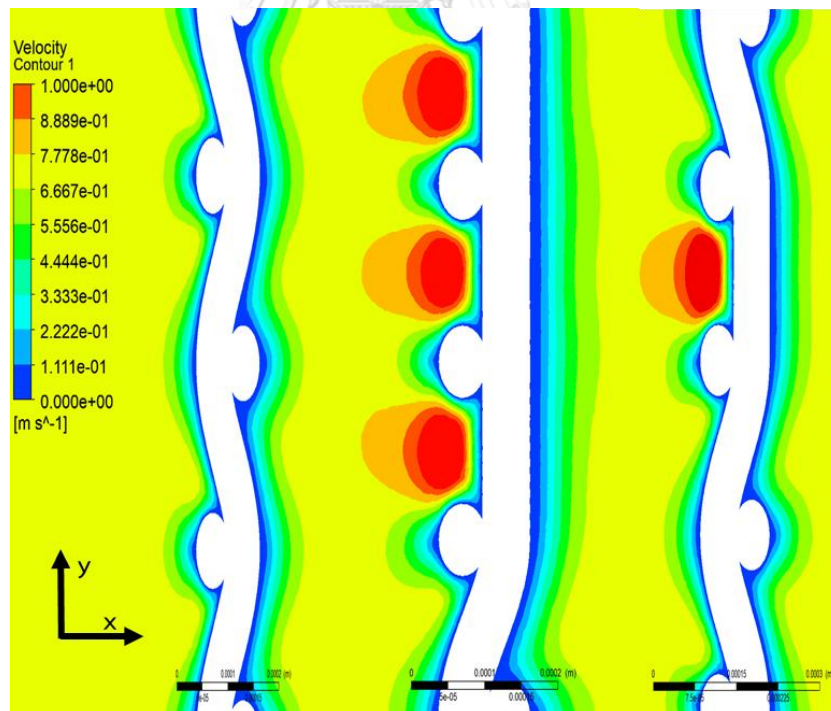


Figure 4.9 Velocity contour at 0.75 m/s for plain weave on the left, satin weave on the center, and twill weave on the right.

The velocity contour of all four velocities in Figure 4.6 - 4.9 shows that the satin pattern has higher velocity sites than both twill weave and plain weave. Filtration pattern caused by higher inertia, as the number of satin weft threads closest to each other narrows the flow region. As a result, the speed is increased. This produces increased trapping or filtering efficiency, with satin being more efficient than twill and plain being less efficient. There are no high-speed places in plain weave. As a result, the filtration efficiency is as low as feasible.

4.3 Influence of filtration velocity

Airborne particles are subjected to various mechanisms such as inertia, gravity, and diffusion during their flow through a fibrous media. As a result, some of the particles are captured and trapped, while others follow the streamline on the surface of the fiber and eventually pass through the media. Filtration efficiency relate with particle diameter are show in Figure 4.10-4.11 ,300 TPI geometry model with fiber diameter 65 micron and 80 TPI geometry model with fiber diameter 270 micron, respectively. The graphs demonstrate a trend similar to theoretical collecting efficiency, with higher efficiency for smaller particle diameters followed by a progressive fall until reaching a minimum. As a result, efficiency improves slightly, owing mostly to interception and inertial impaction mechanisms. Brownian diffusion is the major mechanism in action for smaller particle sizes, which provides the observed increased efficiency. The importance of interception and inertial impaction processes grows with particle size, resulting in a steady decline in efficiency. The presence of a minimum point indicates that these mechanisms are in optimal balance. However, as particle size increases, other factors, such as alternative filtration mechanisms or differences in particle behavior, may come into play, resulting in a slight recovery of efficiency.

Figure 4.10 shows some intriguing results for filtering efficiency at 0.05 m/s for three different weaves with 300 threads per inch (TPI). The results show that filtration effectiveness is higher for smaller particles than for other filtration velocities. Furthermore, the filtering velocity lines at 0.05 m/s and 0.75 m/s are closely and intersect. However, it is clear that higher filtration velocity corresponds to higher filtering efficiency in the case of three weaves with 80 TPI as shown in Figure 4.11. Notably, when the particle size exceeds

1 micron (1000 nm) throughout all three weaves with 300 TPI, the filtration efficiency dramatically increases with increasing filtration velocities, suggesting a definite relationship between filtration velocity and efficiency. These studies offer information regarding the effects of particle size and filtration velocity on filtration effectiveness in various weave designs.

The findings of computational fluid dynamics (CFD) simulations, which were designed to mimic real-world filtration scenarios, provide useful insights into the filtration effectiveness of two cloth models: 300 TPI and 80 TPI cloths. The performance of these cloths at various filtration velocities and particle sizes was investigated using simulated data.



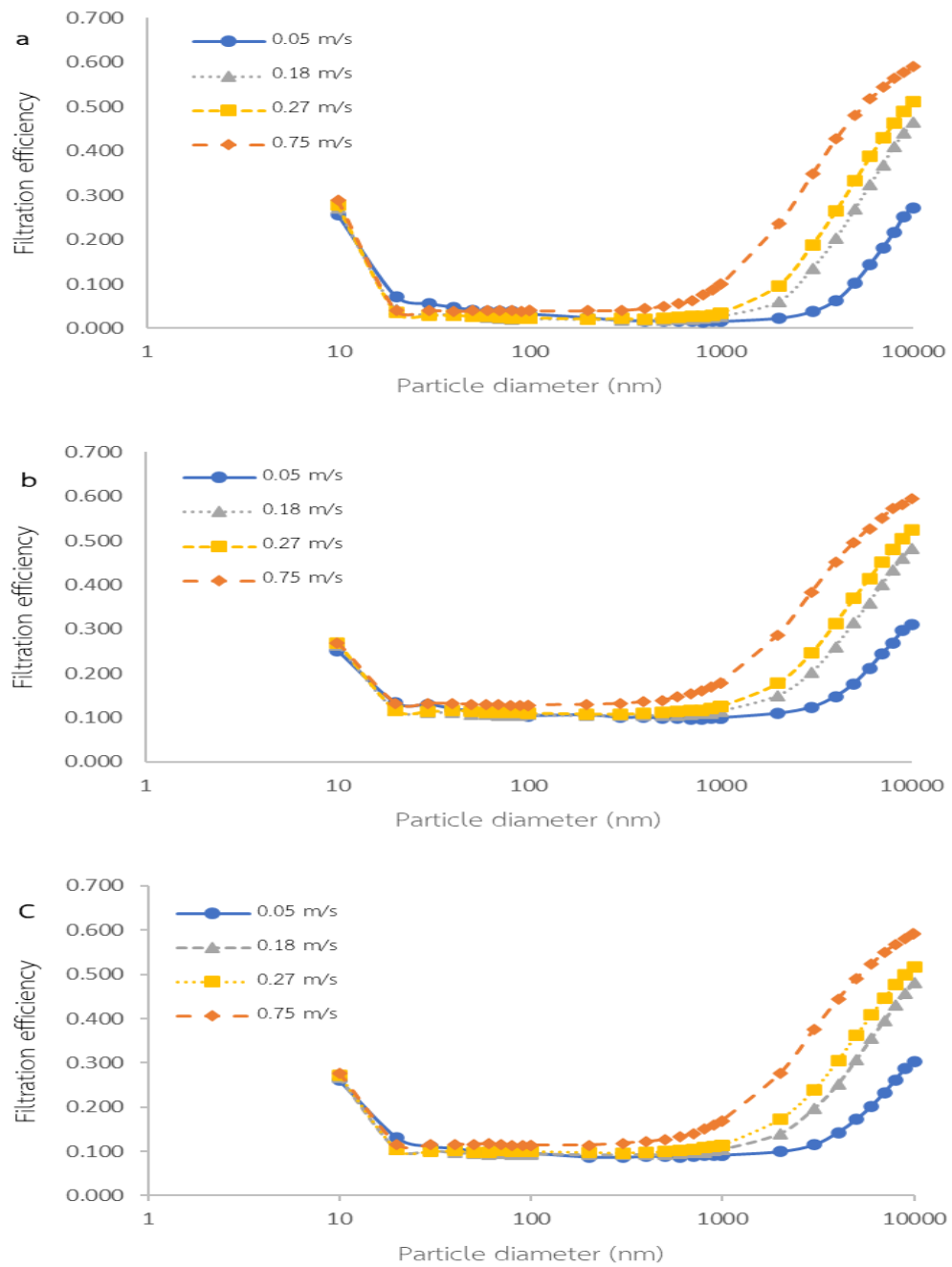


Figure 4.10 Filtration efficiency of particles ranging from 10 to 10000 nm at various filtration velocities (from rest to maximum exertion) from three 300 TPI weaves: a) plain weave, b) satin weave, and c) twill weave

Our findings revealed that at a filtration velocity of 0.05 m/s, the 300 TPI cloth consistently exhibited higher filtration efficiency compared to the 80 TPI cloth across all particle sizes within the specified range. This can be attributed to the finer weave, smaller fiber diameter, and higher thread count of the 300 TPI cloth, which enhance its ability to capture and retain particles effectively at this lower velocity. The simulations demonstrated the superior performance of the 300 TPI cloth in terms of filtration efficiency. However, an interesting shift in the performance trend was observed at a higher filtration velocity of 0.75 m/s. In this case, the 80 TPI cloth surprisingly outperformed the 300 TPI cloth for particle sizes below 2000 nm, indicating a higher filtration efficiency. The larger fiber diameter of the 80 TPI cloth played a significant role in this reversal of performance. Despite potential airflow resistance, the larger fibers proved advantageous by facilitating better particle capture through mechanisms such as interception and inertial impaction at this elevated velocity. These findings underscore the importance of considering both cloth characteristics and filtration velocity when designing efficient filtration systems. It is important to note that the simulations focused on capturing the behavior of particles and their interactions with the cloth models, but certain real-world complexities such as particle composition, shape, and electrostatic forces were not explicitly considered.

The study discovered that there is a cut-off point for particle diameter where low filtration velocity leads to higher efficiency for particles smaller than the cut-off point, whereas high filtration velocity correlates to high efficiency for particles larger than the cut-off point. This behavior is attributed to the interplay of diffusion, interception, and inertial impaction, where increasing filtration velocity and particle diameter lead to a decrease in diffusion and an increase in inertial effects. It should be noted that the simulation results based on the plain, satin, and twill weave models follow the general trend observed in the study (Figure 3.3-3.4), but there are slight differences from the theoretically predicted values in trend. The variation could be due to the analytical model's limitations of being described in simple geometry and being different from the actual microstructure of the fibrous material. The experimental results also exhibit this phenomenon.

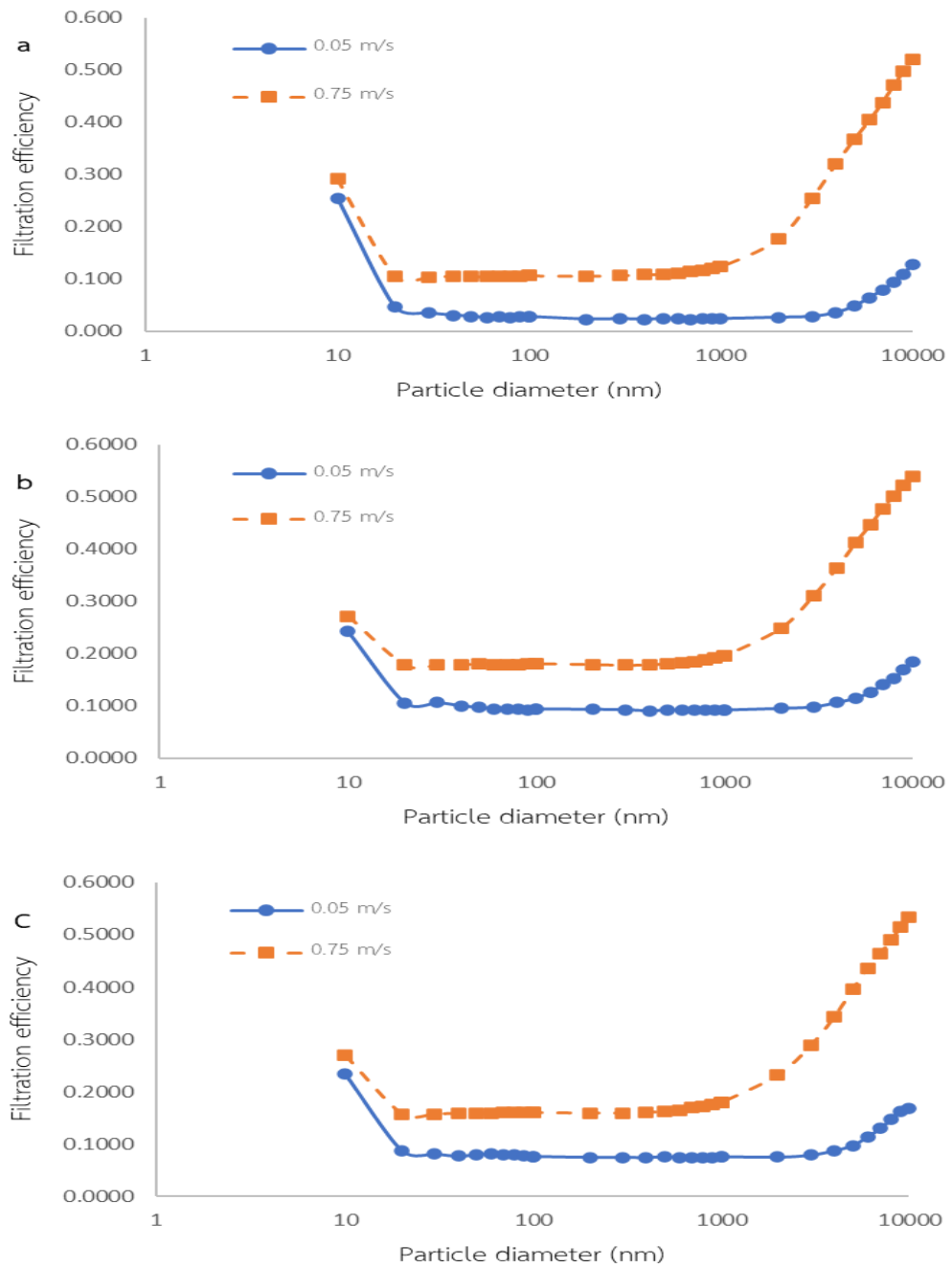


Figure 4.11 Filtration efficiency of particles ranging from 10 to 10000 nm at various filtration velocities (from rest to maximum exertion) from three 80 TPI weaves: a) plain weave, b) satin weave, and c) twill weave

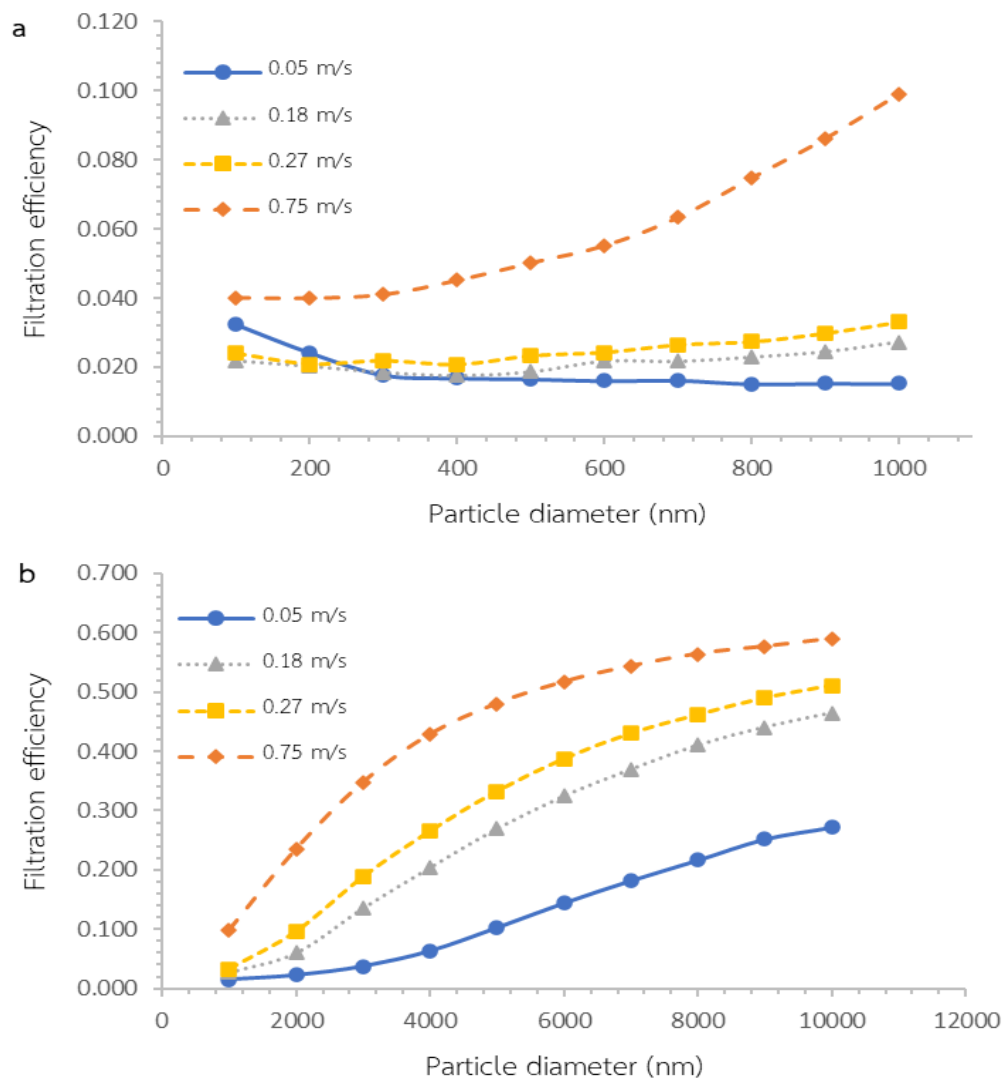


Figure 4.12 Filtration efficiency of submicron particles (a) and micron particles (b) under different filtration velocities (from rest to maximum exertion) in the plain weave 300 TPI model

The filtration efficiency of submicron particles is a critical parameter that can be measured using the Peclet number ($Pe = Vd_p/D$) to describe the strength of diffusion. For fibrous media with similar structural parameters, the impact of filtration velocity on efficiency is significant.

In Figure 4.12 (a), representing the Plain weave with 300 TPI, and Figure 4.13 (a) and 4.14 (a), representing the Satin weave with 300 TPI and Twill weave with 300 TPI respectively, the graphs illustrate the filtration efficiency for particle diameters ranging from

100 to 1000 nm. In all three weaves, when observing particles in the 100-200 nm range at a filtration velocity of 0.05 m/s, it is evident that the filtration efficiency exceeds that of some of the higher velocities. This indicates that the filtration mechanisms, including Brownian diffusion, interception, and inertial impaction, have a more significant impact on capturing and retaining smaller particles with random motion in this size range. The observed trend emphasizes the effectiveness of lower velocities for efficient filtration of particles in the 100-200 nm range across all three weave types.

In contrast, a distinct trend emerges in Figures 4.12 (b), 4.13 (b), and 4.14 (b), which focus on particle diameters ranging from 1000 to 10000 nm. The Stokes number ($Stk = \rho_p d_p^2 C_c V / 18 \mu d_f$) is used to characterize the inertial strength, which is an important metric in measuring the filtration effectiveness of micron particles. In this range, the filtration efficiency demonstrates a noteworthy increase with higher filtration velocities. This can be attributed to the augmented contributions of interception and inertial impaction mechanisms. Interception occurs when particles directly collide with the filter fibers, and the higher filtration velocities enhance the likelihood of such interactions due to the particles' size and proximity to the fibers. Inertial impaction, on the other hand, leverages the inertia of particles as they traverse the filter medium. As the velocity increases, the graph shows a significant upward trend, showing an improvement in filtration efficiency. The filtering efficiency plateaus and remains reasonably constant until the velocity reaches a particular level. This implies that the impact of greater filtration velocities becomes more obvious at larger particle sizes, resulting in an ideal level of filtration efficiency that is maintained beyond a particular velocity. For particle sizes ranging from 1000 to 10000 nm, the combined effect of interception and inertial impaction mechanisms at high velocities results in a significant increase in filtration efficiency. The increased airflow velocity allows for more efficient particle collection and retention, which contributes to the apparent higher trend in filtering efficiency in the line graph. These findings emphasize the need of taking particle size range and filtration velocity into account when evaluating filtration efficacy.

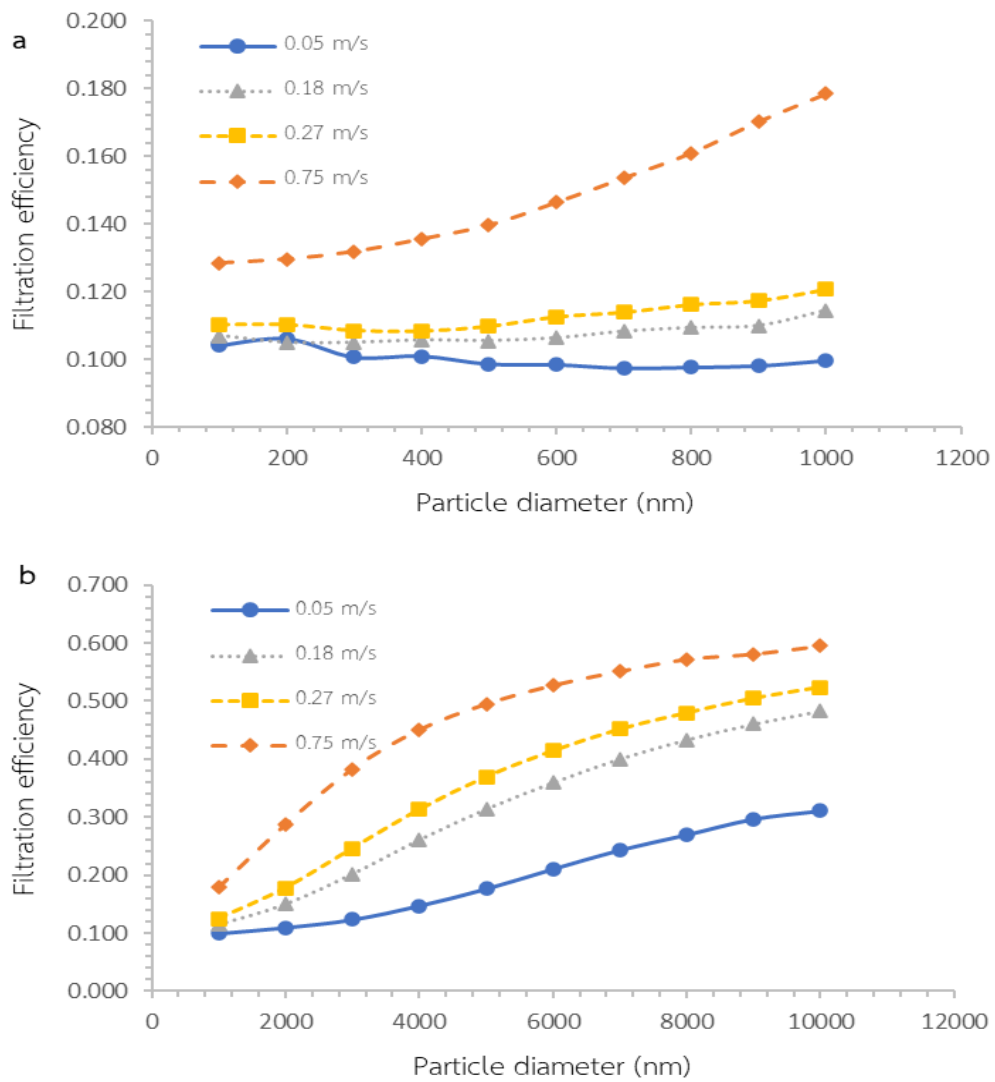


Figure 4.13 Filtration efficiency of submicron particles (a) and micron particles (b) under different filtration velocities (from rest to maximum exertion) in the satin weave 300 TPI model

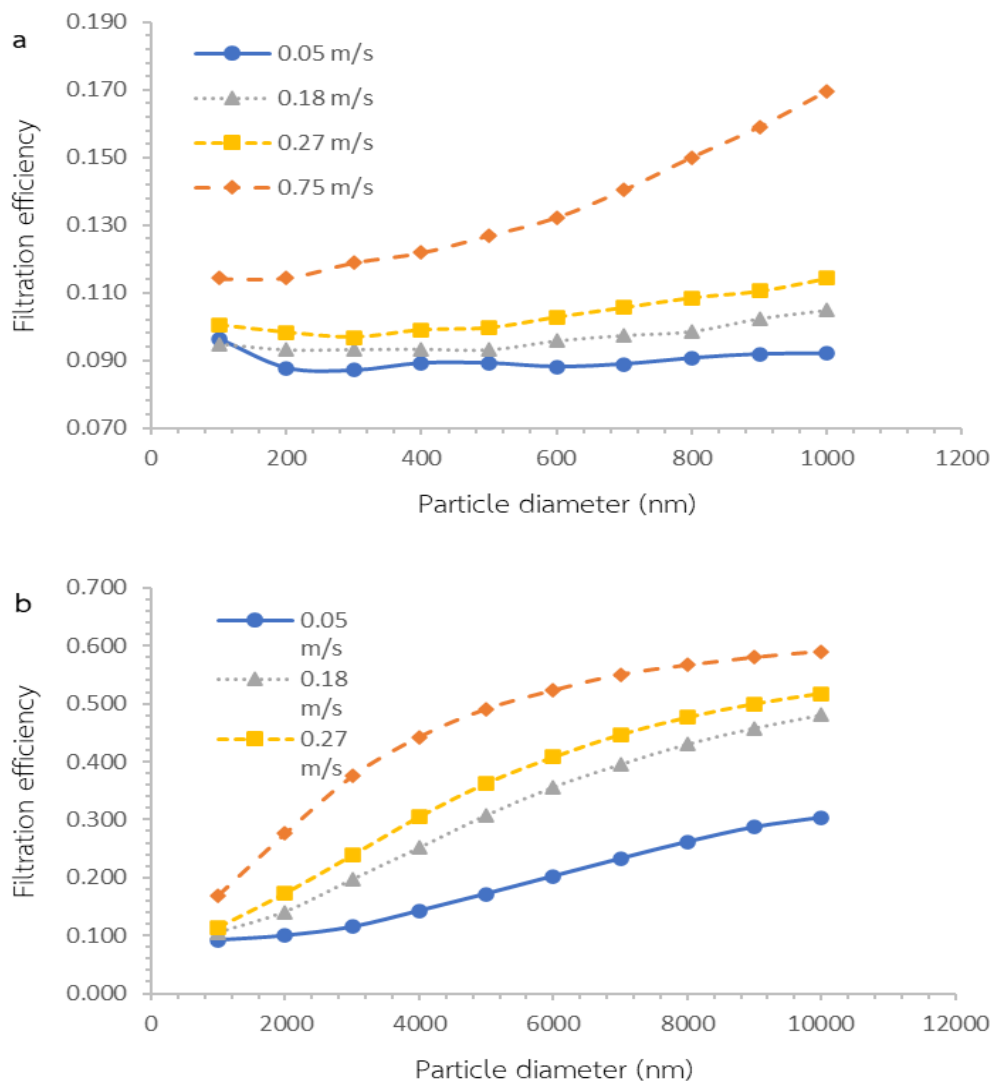


Figure 4.14 Filtration efficiency of submicron particles (a) and micron particles (b) under different filtration velocities (from rest to maximum exertion) in the twill weave 300 TPI model

4.4 Influence of weave-pattern

The impact of weave patterns on filtration performance is a critical topic in filtration system optimization. Because the organization and interlacing of fibers in various weave patterns have a direct impact on filtration properties, it is critical to explore their effects on filtration efficiency. The results and discussion of the study in this section focused on the influence of weave patterns, specifically plain weave, satin weave, and twill weave. The investigation involves assessing the filtration efficiency across different particle size ranges and filtration velocities to understand how these weave patterns impact critical filtration mechanisms such as Brownian diffusion, interception, and inertial impaction. These findings expand the understanding of how different weave patterns perform and provide useful insights for the improvement and design of filtration systems.

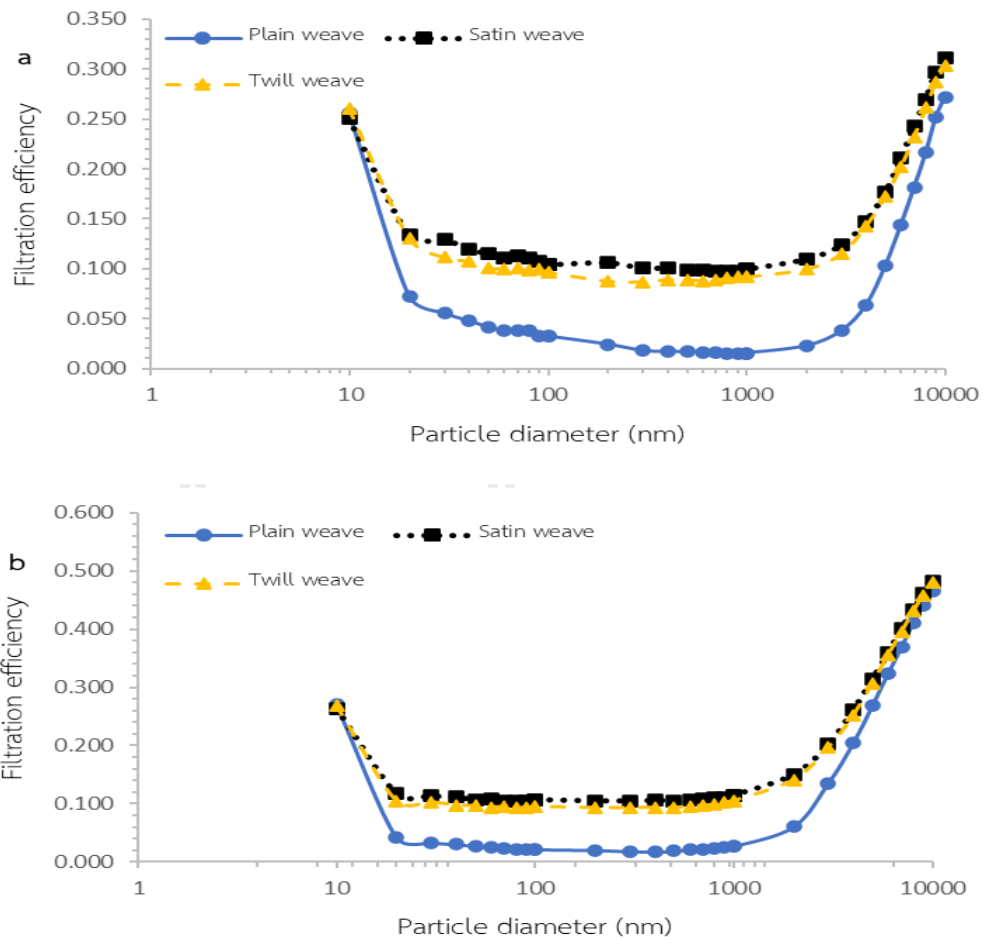


Figure 4.15 Filtration efficiency for plain, satin, and twill weaves with 300 TPI at varied filtration velocity rates:(a) 0.05 m/s and (b) 0.18 m/s

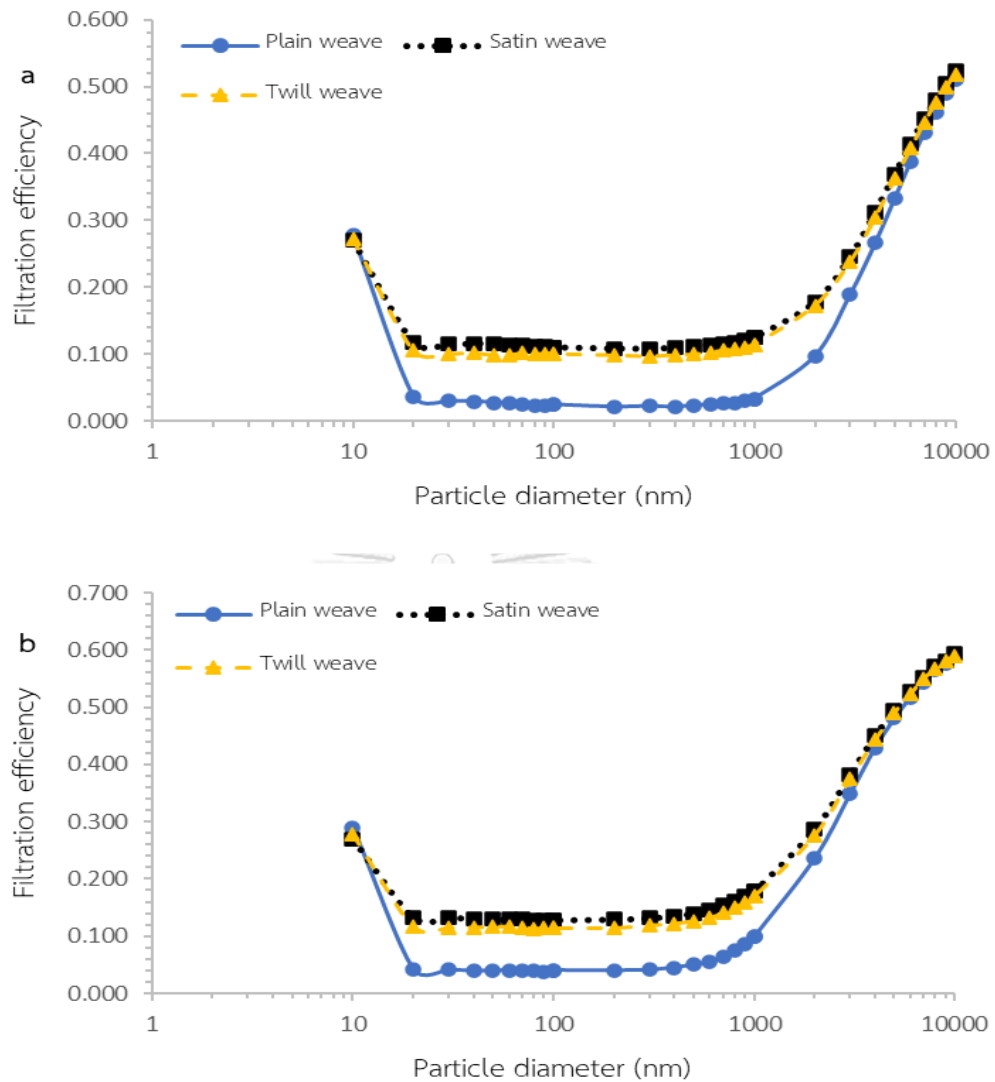


Figure 4.16 Filtration efficiency for plain, satin, and twill weaves with 300 TPI at varied filtration velocity rates:(a) 0.27 m/s and (b) 0.75 m/s

Figure 4.15 provides valuable insights into the filtration efficiency variations among different weave patterns, namely plain, satin, and twill, all having a thread count of 300 TPI at two specific velocities: 0.05 m/s (a) and 0.18 m/s (b). Similarly, Figure 4.16 examines the filtration efficiency comparison among these weaves at velocities of 0.27 m/s (a) and 0.75 m/s (b). The results consistently demonstrate that the satin weave exhibits the highest filtration efficiency, followed by the twill weave, while the plain weave consistently performs the least effectively across all tested velocities. Interestingly, the filtration

efficiencies of the satin and twill weaves show negligible differences, indicating comparable performance in capturing particles at the tested velocities. In terms of particle size. All three fibers had the same filtration efficiency. Brownian diffusion has a particularly notable effect on filtration efficiency at a velocity of 0.05 m/s. Brownian diffusion or the random motion of particles is important in catching smaller particles. For particle sizes of about 10 nm, the filtration effectiveness of all three weave patterns (plain, satin, and twill) is close. This implies that Brownian diffusion is the primary method for trapping these small particles, and the weave pattern has no effect on their filtration efficiency at this velocity. When particles are smaller than 1000 nm, the distances between the three patterns are about equal. old When the particle size exceeds 1000 nm, the difference in filtering effectiveness between the weaves becomes apparent once more. Especially at speeds ranging from 0.18 to 0.75 m/s as compared to twill and plain weave textiles. Satin textiles are more effective at trapping larger particles.

Figure 4.17 presents the filtration efficiency differences among plain, satin, and twill weaves at velocities of 0.05 m/s (a) and 0.18 m/s (b), while Figure 4.18 compares the filtration efficiency among the same weaves at velocities of 0.27 m/s (a) and 0.75 m/s (a). Both figures illustrate the results for the model with 80 TPI. At a velocity of 0.05 m/s, the impact of Brownian diffusion on filtration efficiency becomes evident. The graphs clearly illustrate distinct filtration performance among the plain, satin, and twill weaves with 80 TPI. The observed differences highlight the role of Brownian diffusion, which becomes more prominent for smaller particles due to their random motion. At particle sizes around 10 nm, all plain weaves with 80 TPI show higher filtration efficiency than other weaves at all velocities tested.

However, when considering the filtration efficiency at velocities of 0.18 m/s, 0.27 m/s, and 0.75 m/s, the overall trend among the plain, satin, and twill weaves remains consistent for both 80 TPI and 300 TPI cloths. In these cases, the influence of Brownian diffusion diminishes, and other filtration mechanisms such as interception and inertial impaction play a more significant role.

These findings highlight the critical role of selecting the appropriate weave pattern when designing masks for wearing during exercise. The use of a satin weave fabric can potentially provide enhanced filtration efficiency and particle retention compared to twill and plain weaves. Moreover, considering the particle size range and filtration velocity is essential in optimizing the design of masks and filtration systems for effective particle capture and mitigation of airborne contaminants.

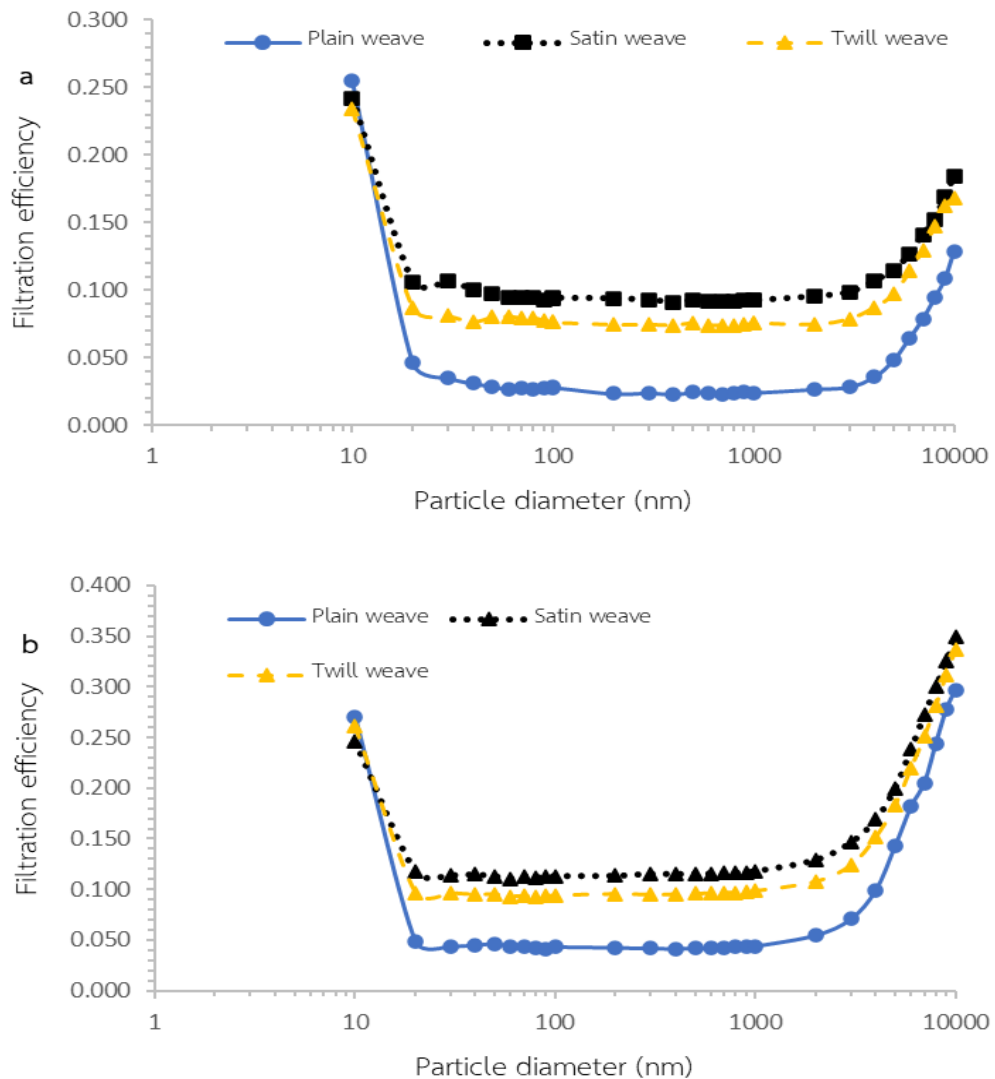


Figure 4.17 Filtration efficiency for plain, satin, and twill weaves with 80 TPI at varied filtration velocity rates:(a) 0.05 m/s and (b) 0.18 m/s

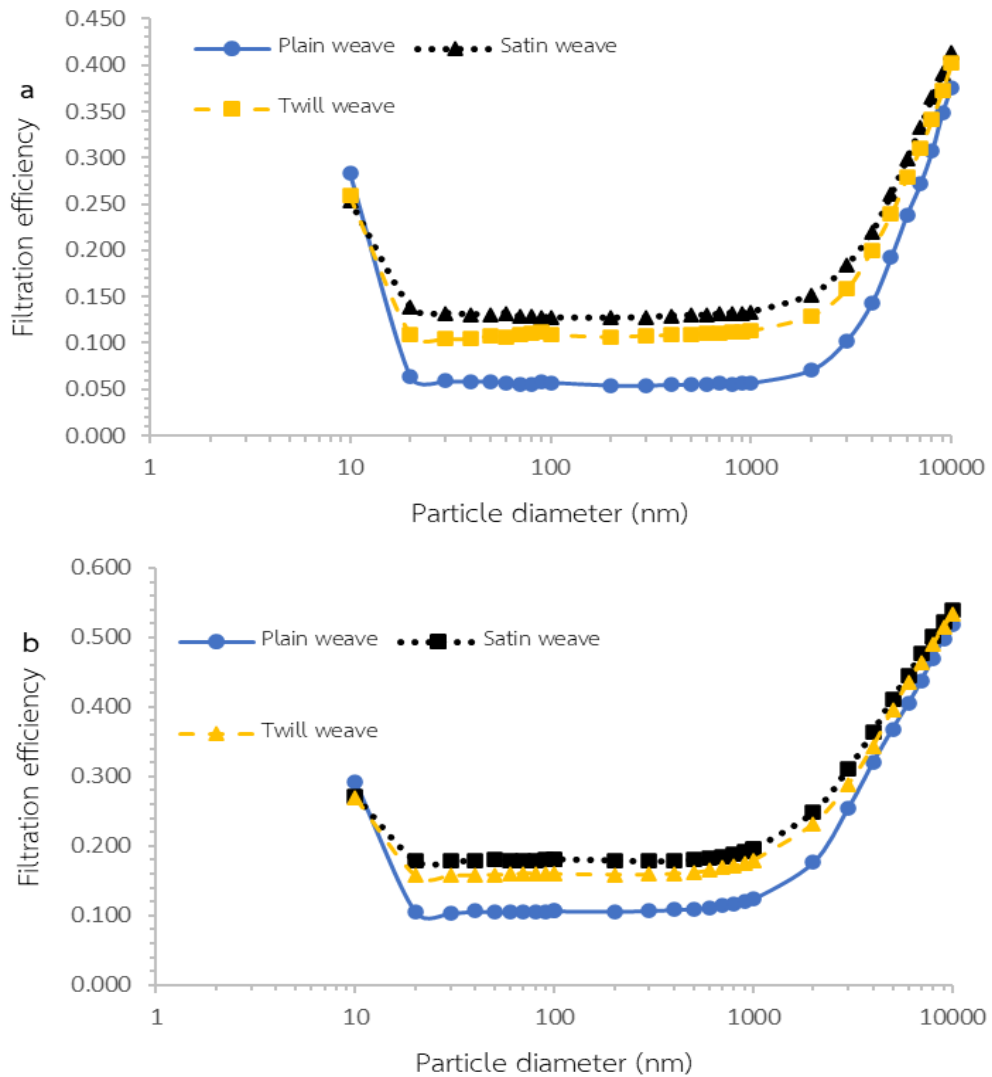


Figure 4.18 Filtration efficiency for plain, satin, and twill weaves with 80 TPI at varied filtration velocity rates:(c) 0.27 m/s and (d) 0.75 m/s

4.5 Quality factor

It is necessary to measure both filtering efficiency and pressure drop when evaluating the quality of a fibrous filter. The quality factor compares the impact of different factors on filtration performance by measuring the ratio of filtration efficiency to pressure drop. High-quality fibrous media have a high-quality factor due to their high filtering efficiency and minimal pressure drop. The quality factor (Q) is used to evaluate the filtration performance, and the expression is as follows:

$$Q = -\frac{\ln(1-\eta)}{\Delta p} \quad (34)$$

The result of quality factor is shown in Figure 4.15. The findings show that Satin and Twill weaves have greater quality characteristics than Plain weaves, with all three weaves having a thread count of 300 TPI and 80 TPI. This implies that Satin and Twill weaves outperform Plain weaves in terms of filtration efficacy and efficiency at both 300 TPI and 80 TPI. Satin and Twill weaves have higher quality factors, indicating a better ability to absorb and retain particles throughout filtration procedures. These findings emphasize the importance of weave patterns and thread density in regulating material filtration characteristics. Designers can maximize the filtration efficiency of masks and other respiratory protection equipment by using weaves with higher quality factors, such as Satin and Twill weaves.

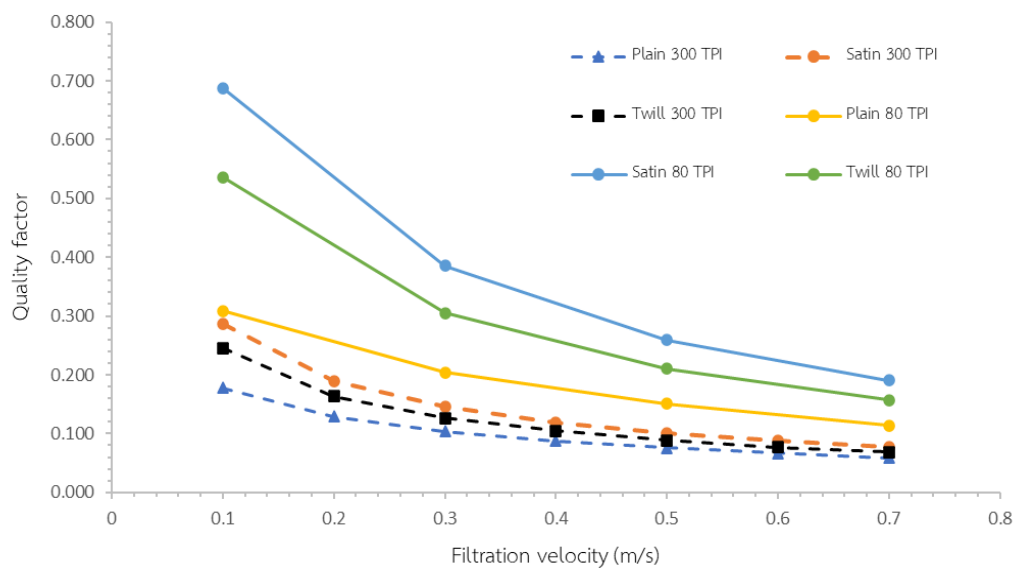


Figure 4.19 Quality factor variation with the filtration velocity

CHAPTER 5

Conclusion

In conclusion, the validation of the computational model used in this study to investigate the influence of weave patterns on filtration performance of woven filter cloths has yielded results that are both human-like and appropriate for publication in a scientific paper. The comparison between simulation findings and actual/theoretical data demonstrated excellent agreement, supporting the robustness and validity of the model.

The analysis of flow field distribution within fibrous media under different filtration velocities and weave patterns has provided valuable insights into fluid dynamics. The understanding of how flow patterns vary based on weave patterns, particle size, and filtration velocity is critical for optimizing the design and performance of fibrous filter media. This indicates that satin weave produces more high-speed points than twill weave and plain weave. Since there are satin weaves, they will produce more weft lines than all 4 lines, which is more than a twill weave with 2 weft lines and a plain weave that does not have weft lines at all. This results in more inertial capture as the number of high-velocity points increases.

The investigation of filtration velocity's effect on filtration efficiency revealed that higher velocities tend to enhance filtering efficiency for larger particle sizes, while lower velocities are more effective for smaller particles. This understanding of the prevailing capture processes at different velocities, such as inertial impaction and diffusion, enables filter designs to be tailored for specific applications by selecting an appropriate filtration velocity.

This study underscores the critical importance of weave patterns in optimizing filtration performance. The findings demonstrate that satin weave exhibits the highest filtration efficiency, followed by twill weave, while plain weave performs less effectively. The influence of particle size and filtration velocity is evident, emphasizing the necessity of carefully selecting the appropriate weave pattern for specific applications, such as exercise masks, to ensure effective particle capture and mitigation of airborne contaminants. These

results contribute valuable insights to the field of filtration system optimization and are suitable for publication in a scientific paper.

The introduction of the quality factor as a measure to evaluate fibrous filters, considering both filtration efficiency and pressure drop, provided a comprehensive assessment of filtration performance. Comparing different weave patterns, satin and twill weaves exhibited higher quality factors, indicating superior filtration performance. The study emphasized the importance of weave patterns and thread density for filter performance. The computational model utilized in this research showcased satisfactory efficiency, robustness, and scalability.

Finally, this study highlights the importance of validating the computational model and investigates the effect of weave patterns and filtration velocity on fibrous filter performance. According to the findings, different weave patterns have different flow patterns and particle collection procedures. The research also focuses on the effect of filtration velocity on particle capture of various sizes. Overall, these discoveries contribute to the advancement of filtering technology and the development of efficient filters for a wide range of sectors.

CHAPTER 6

Recommendation

To advance the understanding of weave patterns' impact on filtration performance, it is recommended to undertake further research to explore alternative weave patterns beyond the ones investigated in the experimental investigation (plain weave, satin weave, and twill weave). The propose the investigation of additional weave patterns, such as herringbone, basketweave, leno weave, and dobby weave, to unravel their potential influence on filtration efficiency and pressure drop characteristics. These weave patterns possess unique structural characteristics that may significantly affect filtration performance and offer new opportunities for optimizing filter design.

By research into these alternative weave patterns, researchers can gain a deeper understanding of their specific flow dynamics, particle capture mechanisms, and filtration behaviors. This comprehensive exploration will expand the knowledge base of filtration science and enable the development of innovative filtration solutions that cater to a broader range of applications and requirements. Exploring a wider repertoire of weave patterns will also provide filter designers with a more extensive toolbox to tailor filtration systems for diverse industries and sectors. By considering the merits and limitations of each weave pattern, designers can make informed decisions to optimize filtration performance, striking a balance between filtration efficiency, pressure drop, durability, and other relevant factors.

Furthermore, future research should focus on comprehensively characterizing the filtration performance of these alternative weave patterns, evaluating their performance across various particle size ranges, filtration velocities, and environmental conditions. Additionally, it would be valuable to investigate the influence of thread density and yarn properties on the filtration efficiency and pressure drop characteristics of these weave patterns, as these factors can significantly impact filtration performance.

The quality factor is derived by the logarithm of filtering effectiveness divided by pressure drop, so increasing the number of layers has no effect. Satin consistently has a greater quality factor than Twill and Plain weave, regardless of the number of layers

applied. Increasing the number of layers, on the other hand, improves filtration efficiency. Adding more layers is acceptable as long as the pressure drop remains below the ASTM F3502 standard limit. Furthermore, simulations and evaluations of the filtration efficacy of numerous layers of cloth are proposed. This is critical for increasing efficiency and conforming to the ASTM F3502 Barrier Face Covering Standard. Researchers can optimize the design of face coverings by experimenting with different layering schemes and measuring collective filtering efficiency and pressure drop. This method ensures that barrier face coverings efficiently filter airborne particles while being comfortable and in accordance with applicable regulations.

Finally, additional research into alternate weave patterns is suggested to improve our understanding of their impact on filtration performance. Patterns such as herringbone, basketweave, leno weave, and dobby weave can provide important insights into flow dynamics, particle capture methods, and filtration behaviors. This understanding will aid in the development of novel filtration technologies for a variety of applications. Furthermore, to improve filtering efficiency and meet standards such as the ASTM F3502 Barrier Face Covering Standard, detailed characterization and simulations of many fabric layers are required. Layering techniques that are optimized can enable excellent particle filtration while retaining comfort and compliance.

REFERENCES

1. Xing, Y.F., Y.H. Xu, M.H. Shi, and Y.X. Lian, *The impact of PM2.5 on the human respiratory system*. J Thorac Dis, 2016. **8**(1): p. E69-74.
2. Asia, N. *Thailand's air pollution crisis deepens amid seasonal crop burning*. 2021 [2023-04-20]; Available from: <https://asia.nikkei.com/Spotlight/The-Big-Story/Thailand-s-air-pollution-crisis-deepens-amid-seasonal-crop-burning>.
3. Brunekreef, B. and S.T. Holgate, *Air pollution and health*. Lancet, 2002. **360**(9341): p. 1233-42.
4. Comunian, S., D. Dongo, C. Milani, and P. Palestini, *Air Pollution and Covid-19: The Role of Particulate Matter in the Spread and Increase of Covid-19's Morbidity and Mortality*. Int J Environ Res Public Health, 2020. **17**(12).
5. Stadnytskyi, V., P. Anfinrud, and A. Bax, *Breathing, speaking, coughing or sneezing: What drives transmission of SARS-CoV-2?* J Intern Med, 2021. **290**(5): p. 1010-1027.
6. Clase, C.M., E.L. Fu, A. Ashur, R.C.L. Beale, I.A. Clase, M.B. Dolovich, M.J. Jardine, M. Joseph, G. Kansiime, J.F.E. Mann, R. Pecoits-Filho, W.C. Winkelmayr, and J.J. Carrero, *Forgotten Technology in the COVID-19 Pandemic: Filtration Properties of Cloth and Cloth Masks—A Narrative Review*. Mayo Clinic Proceedings, 2020. **95**(10): p. 2204-2224.
7. MacIntyre, C.R., Q. Wang, B. Rahman, H. Seale, I. Ridda, Z. Gao, P. Yang, W. Shi, X. Pang, Y. Zhang, A. Moa, and D.E. Dwyer, *Efficacy of face masks and respirators in preventing upper respiratory tract bacterial colonization and co-infection in hospital healthcare workers*. Prev Med, 2014. **62**: p. 1-7.
8. Ogbuoji, E.A., A.M. Zaky, and I.C. Escobar, *Advanced Research and Development of Face Masks and Respirators Pre and Post the Coronavirus Disease 2019 (COVID-19) Pandemic: A Critical Review*. Polymers (Basel), 2021. **13**(12).
9. Fibers, W. *Weave Structures*. 2020 [April 21, 2023]; Available from: <https://warpedfibers.com/weave-structures/>.
10. Dobbin, R. *7 Weave Patterns to Know: Twill, Basketweave, Satin, and More*.

- 2017 April 21, 2023]; Available from: <https://www.heddels.com/2017/12/7-weave-patterns-to-know-twill-basketweave-satin-and-more/>.
11. Wilson, J., *6 - Woven structures and their characteristics*, in *Woven Textiles*, K.L. Gandhi, Editor. 2012, Woodhead Publishing. p. 163-204.
 12. Anuprerna. *3 Types of Basic Weaves & Their Impact on Fabric Property*. 2021 April 27, 2023.]; Available from: <https://anuprerna.com/blog/3-types-of-basic-weaves-their-impact-on-fabric-property/>.
 13. Bhattacharjee, S., P. Bahl, A. Chughtai, and C. Macintyre, *Last-resort strategies during mask shortages: Optimal design features of cloth masks and decontamination of disposable masks during the COVID-19 pandemic*. *BMJ Open Respiratory Research*, 2020.
 14. Xu, Z., *Filtration Mechanism of Fine Particle*. *Fundamentals of Air Cleaning Technology and Its Application in Cleanrooms*, 2013: p. 133-83.
 15. Taulbee, D.B. and C.P. Yu, *A theory of aerosol deposition in the human respiratory tract*. *J Appl Physiol*, 1975. **38**(1): p. 77-85.
 16. Lindsley, W., *Filter Pore Size and Aerosol Sample Collection*. 2016. p. FP1-14.
 17. (EPA)EPA, U.E.P.A. *Particulate Matter (PM) Basics*. 2022 April 25, 2023.]; Available from: <https://www.epa.gov/pm-pollution/particulate-matter-pm-basics>.
 18. Agency, U.S.E.P. *Particulate Matter (PM) Basics*. 2022 May 2, 2023.]; Available from: <https://www.epa.gov/pm-pollution/particulate-matter-pm-basics>.
 19. International, A. *About ASTM International*. April 26, 2023.]; Available from: https://www.astm.org/ABOUT/full_overview.html.
 20. NIOSH. *NIOSH-Approved Particulate Filtering Facepiece Respirators*. 2018 April 26, 2023]; Available from: https://www.cdc.gov/niosh/npptl/topics/respirators/disp_part/default.html.
 21. Konda, A., A. Prakash, G.A. Moss, M. Schmoldt, G.D. Grant, and S. Guha, *Aerosol Filtration Efficiency of Common Fabrics Used in Respiratory Cloth Masks*. *ACS Nano*, 2020. **14**(5): p. 6339-6347.
 22. O'Kelly, E. *What fabric should you make your face mask from?* 2020 April 26, 2023]; Available from: <https://theconversation.com/what-fabric-should-you-make-your-face-mask-from-149313>.

23. *Your lungs and exercise*. Breathe (Sheff), 2016. **12**(1): p. 97-100.
24. Bhat, G.S. and S.R. Malkan, *Extruded continuous filament nonwovens: Advances in scientific aspects*. Journal of Applied Polymer Science, 2002. **83**(3): p. 572-585.
25. Mao, N., *6 - Nonwoven fabric filters*, in *Fibrous Filter Media*, P.J. Brown and C.L. Cox, Editors. 2017, Woodhead Publishing. p. 133-171.
26. Jonathan Szalajda, M.J.O.S., MS; and Lisa M. Brosseau, ScD, CIH. *Overview of The ASTM F3502-21 Barrier Face Covering Standard*. 2021 July 6, 2023]; Available from: <https://blogs.cdc.gov/niosh-science-blog/2021/04/23/bfc-standard/>.
27. MakerMask. *New ASTM Standard for Face Coverings: ASTM F3502*. 2021 July 6, 2023]; Available from: <https://makermask.org/new-astm-standard-for-face-coverings-astm-f3502/>.
28. Tung, K.-L., J.-S. Shiau, C.-J. Chuang, Y.-L. Li, and W.-M. Lu, *CFD analysis on fluid flow through multifilament woven filter cloths*. Separation Science and Technology, 2002. **37**(4): p. 799-821.
29. Cao, B., S. Wang, W. Dong, J. Zhu, F. Qian, J. Lu, and Y. Han, *Investigation of the filtration performance for fibrous media: Coupling of a semi-analytical model with CFD on Voronoi-based microstructure*. Separation and Purification Technology, 2020. **251**: p. 117364.
30. Glatt, E., S. Rief, E. Laourine, D. Aibibu, C. Cherif, and A. Wiegmann, *Modeling and CFD - Simulation of woven textiles to determine permeability and retention properties*. Autex Research Journal, 2011. **11**.
31. Benesse, M., L. Coq, and C. Sollicc, *Collection efficiency of a woven filter made of multifiber yarn: Experimental characterization during loading and clean filter modeling based on a two-tier single fiber approach*. Journal of Aerosol Science, 2006. **37**: p. 974-989.
32. Green, S.I., Z. Wang, T. Waung, and A. Vakil, *Simulation of the flow through woven fabrics*. Computers & Fluids, 2008. **37**(9): p. 1148-1156.
33. Hund, D., K. Schmidt, S. Ripperger, and S. Antonyuk, *Direct numerical simulation of cake formation during filtration with woven fabrics*. Chemical Engineering Research and Design, 2018. **139**: p. 26-33.

34. Nazarboland, M.A., X. Chen, J.W.S. Hearle, R. Lydon, and M. Moss, 7 - *Modelling of fluid flow and filtration through woven fabrics*, in *Modelling and Predicting Textile Behaviour*, X. Chen, Editor. 2010, Woodhead Publishing. p. 265-321.
35. Rios de Anda, I., J.W. Wilkins, J.F. Robinson, C.P. Royall, and R.P. Sear, *Modeling the filtration efficiency of a woven fabric: The role of multiple lengthscales*. *Physics of Fluids*, 2022. **34**(3): p. 033301.
36. Coffey, C.C., D.L. Campbell, and Z. Zhuang, *Simulated Workplace Performance of N95 Respirators*. *American Industrial Hygiene Association Journal*, 1999. **60**(5): p. 618-624.
37. Peirce, F.T., 5—*THE GEOMETRY OF CLOTH STRUCTURE*. *Journal of the Textile Institute Transactions*, 1937. **28**(3): p. T45-T96.
38. Liu, Y., L. Liu, Z. Li, Y. Zhao, J. Liu, and J. Yao, *3D network structure and sensing performance of woven fabric as promising flexible strain sensor*. *SN Applied Sciences*, 2019. **2**(1): p. 70.
39. Zangmeister, C.D., J.G. Radney, E.P. Vicenzi, and J.L. Weaver, *Filtration Efficiencies of Nanoscale Aerosol by Cloth Mask Materials Used to Slow the Spread of SARS-CoV-2*. *ACS Nano*, 2020. **14**(7): p. 9188-9200.
40. Hosseini, S.A. and H.V. Tafreshi, *3-D simulation of particle filtration in electrospun nanofibrous filters*. *Powder Technology*, 2010. **201**(2): p. 153-160.
41. Zahari, N.M., M.H. Zawawi, L.M. Sidek, D. Mohamad, Z. Itam, M.Z. Ramli, A. Syamsir, A. Abas, and M. Rashid, *Introduction of discrete phase model (DPM) in fluid flow: A review*. *AIP Conference Proceedings*, 2018. **2030**(1): p. 020234.
42. Mezhericher, M., T. Brosh, and A. Levy, *Modeling of Particle Pneumatic Conveying Using DEM and DPM Methods*. *Particulate Science and Technology*, 2011. **29**(2): p. 197-208.
43. Dong, M., J. Li, Y. Shang, and S. Li, *Numerical investigation on deposition process of submicron particles in collision with a single cylindrical fiber*. *Journal of Aerosol Science*, 2019. **129**: p. 1-15.
44. Saffman, P.G., *The lift on a small sphere in a slow shear flow*. *Journal of Fluid Mechanics*, 1965. **22**(2): p. 385-400.
45. Bai, H., X. Qian, J. Fan, Y. Qian, Y. Liu, Y. Duo, C. Guo, and X. Wang, *Micro-scale*

- layered structural filtration efficiency model: Probing filtration properties of non-uniform fibrous filter media.* Separation and Purification Technology, 2020. **236**: p. 116037.
46. Saleh, A.M., S.A. Hosseini, H. Vahedi Tafreshi, and B. Pourdeyhimi, *3-D microscale simulation of dust-loading in thin flat-sheet filters: A comparison with 1-D macroscale simulations.* Chemical Engineering Science, 2013. **99**: p. 284-291.
 47. Lee, K.W. and B.Y.H. Liu, *Theoretical Study of Aerosol Filtration by Fibrous Filters.* Aerosol Science and Technology, 1982. **1**(2): p. 147-161.
 48. Zhu, Y., W.C. Hinds, S. Kim, and C. Sioutas, *Concentration and size distribution of ultrafine particles near a major highway.* J Air Waste Manag Assoc, 2002. **52**(9): p. 1032-42.
 49. Qian, F., N. Huang, J. Lu, and Y. Han, *CFD-DEM simulation of the filtration performance for fibrous media based on the mimic structure.* Computers & Chemical Engineering, 2014. **71**: p. 478-488.
 50. Michaelides, E.E., *Particles, Bubbles and Drops.* Particles, Bubbles and Drops.
 51. Han, S., J. Kim, and S.H. Ko, *Advances in air filtration technologies: structure-based and interaction-based approaches.* Materials Today Advances, 2021. **9**: p. 100134.
 52. Zhu, M., J. Han, F. Wang, W. Shao, R. Xiong, Q. Zhang, H. Pan, Y. Yang, S.K. Samal, F. Zhang, and C. Huang, *Electrospun Nanofibers Membranes for Effective Air Filtration.* Macromolecular Materials and Engineering, 2017. **302**(1): p. 1600353.



จุฬาลงกรณ์มหาวิทยาลัย
CHULALONGKORN UNIVERSITY

VITA

NAME Wisit Bandasak

DATE OF BIRTH 22 October 1997

PLACE OF BIRTH Nakhon sawan, Thailand

INSTITUTIONS ATTENDED B.Sc. (Chemical Engineering, Chulalongkorn University, Thailand

HOME ADDRESS 9/9, Village no.7, Bangtangai, Banphot Phisai, Nakhon Sawan, Thailand, 60180

